

Published in *Advances in Molecular Vibrations and Collision Dynamics* 1A, 1 (1990). However, the published version had many typographical errors. This is the version that was submitted to the journal, and is much more accurate.

An Introduction to the Dynamics of Van der Waals Molecules

Jeremy M. Hutson

Department of Chemistry, University of Durham, South Road, Durham, DH1 3LE, England

OUTLINE

1. Introduction
2. Atom–atom Van der Waals Molecules
 - 2.1 Numerical Methods
 - 2.2 Spectroscopic Constants
3. Atom–diatom Van der Waals Molecules
 - 3.1 Representation of the Intermolecular Potential
 - 3.2 The Coupled Equations
4. Approximate Methods
 - 4.1 Angular Momentum Coupling Cases
 - 4.2 Centrifugal Decoupling or Helicity Decoupling
 - 4.3 Distortion Approximations
 - 4.4 Perturbation Theory
 - 4.5 Adiabatic Approximations
5. Dipole Moments and Spectroscopic Intensities
 - 5.1 Space-fixed
 - 5.2 Body-fixed
6. Larger Systems
 - 6.1 Atom–polyatom Systems
 - 6.2 Molecule–molecule Systems
 - 6.3 Trimeric Systems

Acknowledgments

References

1. Introduction

Van der Waals molecules are complexes formed from pairs of chemically stable neutral molecules. Studies of their structure and dynamics can provide detailed information on anisotropic intermolecular potentials, and they provide valuable prototypes for the large-amplitude motions found in reacting systems. They are readily formed in molecular beams, and an enormous variety of spectroscopic experiments has been carried out on them. There has also been a great deal of theoretical work, aimed at interpreting experimental spectra and understanding the dynamics. However, the theoretical literature in this area draws heavily on scattering theory, and there is no introductory treatment of the subject available. The purpose of this article is to describe the basic theory of Van der Waals molecules, without assuming a knowledge of the scattering literature, and to describe some of the most important results. The emphasis will be on describing the theoretical methods used to calculate vibration-rotation states of Van der Waals molecules, and the coupling schemes and sets of quantum numbers that should be used to describe the resulting states.

Earlier reviews in this area include those of Howard [1], Ewing [2] and Le Roy and Carley [3]; however, all these are now rather dated. Experimental studies of Van der Waals spectra [4,5], their use to determine intermolecular forces [6,7] and the photodissociation of Van der Waals molecules [8] are outside the scope of this article.

The structure of this article is as follows: Section 2 describes atom–atom Van der Waals molecules and the computational methods used for calculating their vibration-rotation energy levels. Sections 3–5 discuss the theory of atom–diatom complexes: section 3 derives the (exact) coupled equations in both space-fixed and body-fixed coordinates; section 4 describes approximate methods, and discusses the different angular momentum coupling cases that can occur; and section 5 describes the factors influencing the intensities of spectroscopic lines. Finally, section 6 gives a brief discussion of larger Van der Waals complexes, and indicates how the methods used for atom–diatom complexes can be generalised.

2. Atom–atom Van der Waals molecules

The simplest Van der Waals molecules are those formed between two closed-shell atoms, A and B, with nuclear masses m_A and m_B . Within the electronic Born-Oppenheimer approximation, the potential energy for a system of this type depends only on the internuclear separation R , and the Hamiltonian for nuclear motion, after separating out the motion of the centre of mass, is

$$H = -\frac{\hbar^2}{2\mu}\nabla^2 + V(R), \quad (1)$$

where μ is the reduced mass, $\mu = m_A m_B / (m_A + m_B)$, and $V(R)$ is the intermolecular potential energy. In spherical polar coordinates the Laplacian is

$$\nabla^2 = R^{-1} \left(\frac{\partial^2}{\partial R^2} \right) R - \frac{\hat{l}^2}{R^2} \quad (2)$$

where

$$\hat{l}^2 = -\frac{1}{\sin^2 \beta} \left[\sin \beta \frac{\partial}{\partial \beta} \left(\sin \beta \frac{\partial}{\partial \beta} \right) + \frac{\partial^2}{\partial \alpha^2} \right] \quad (3)$$

is the angular momentum operator for end-over-end rotation of the nuclei. The two Euler angles α and β are the spherical polar coordinates of the internuclear vector \mathbf{R} relative to a Cartesian axis system fixed in space [$(\beta, \alpha) \equiv (\theta, \phi)$ in the usual notation]. The Schrödinger equation involving the diatomic molecule Hamiltonian is thus separable, and its solutions may be written

$$\psi_{nlm_l} = R^{-1} \chi_{nl}(R) Y_{lm_l}(\beta, \alpha). \quad (4)$$

In this equation, n is a stretching quantum number for the Van der Waals bond, l is the angular momentum quantum number for the rotation of the nuclei, and m_l is the projection of l onto the space-fixed Z axis. The functions $Y_{lm_l}(\beta, \alpha)$ are spherical harmonics [9] satisfying the equation

$$\hat{l}^2 Y_{lm_l}(\beta, \alpha) = l(l+1) Y_{lm_l}(\beta, \alpha). \quad (5)$$

Note that the definition of \hat{l}^2 used here does not include a factor of \hbar^2 , so that the eigenvalues of angular momentum operators are pure numbers. This convention is commonly used in the published literature, but is not universal.

Substitution of equations (1) – (5) into the total Schrödinger equation gives a one-dimensional equation for the function $\chi_{nl}(R)$,

$$\left[-\frac{\hbar^2}{2\mu} \frac{d^2}{dR^2} + V(R) + \frac{\hbar^2 l(l+1)}{2\mu R^2} - E_{nl} \right] \chi_{nl}(R) = 0. \quad (6)$$

Since ψ_{nlm_l} must be finite at $R = 0$ and become zero as $R \rightarrow \infty$ for bound states, the boundary conditions on $\chi_{nl}(R)$ are

$$\begin{aligned} \chi_{nl}(R) &= 0 \text{ at } R = 0 \\ \chi_{nl}(R) &= \text{finite as } R \rightarrow \infty. \end{aligned} \quad (7)$$

In practice, $\chi_{nl}(R)$ decreases exponentially with R as $R \rightarrow \infty$ for bound states because of the form of equation (6). The eigenvalues E_{nl} obtained by solving this equation are also the eigenvalues of the full Hamiltonian of equation (1).

2.1 Numerical methods

There are several methods available for solving one-dimensional Schrödinger equations such as (6). For a few simple model problems, such as the harmonic oscillator and the Morse oscillator, the rotationless problem ($l = 0$) can be solved analytically, but for most potentials of practical interest this is not possible and it is necessary to use numerical methods.

An obvious approach is to use a basis set expansion for $\chi_{nl}(R)$. However, because of the extreme anharmonicity of Van der Waals interaction potentials, a basis set expansion in harmonic oscillator functions is very slowly convergent. In particular, the actual wavefunction often dies off very slowly at large R , and most basis set methods expend a lot of effort in trying to represent this long-range tail in terms of oscillatory basis functions. Various ways around this problem have been proposed: Tennyson and Sutcliffe [10] favour a basis set of Morse-oscillator-like functions, including continuum contributions, and various other workers have used a nonorthogonal basis set of Gaussians functions with centres distributed along the R axis [11].

The most common method of solving equation (6) for Van der Waals complexes is to integrate the differential equation numerically. Solutions satisfying the boundary conditions are propagated from long and short range to a matching distance in the classically allowed region; the two wavefunctions and their derivatives can be made to match only if the energy chosen is an eigenvalue. The strategy used is to integrate the equation first using a guessed eigenvalue, and then to use the extent of the mismatch to make an improved estimate of the eigenvalue; this is known as the shooting method [12]. This procedure can then be iterated until the eigenvalue is known to any desired accuracy.

A wide variety of methods is available for propagating ordinary differential equations such as (6). Cooley [13] proposed the use of Numerov integration, which takes advantage of the absence of first-derivative terms in the one-dimensional Schrödinger equation to obtain an integration formula accurate to the fourth power of the step size. Cooley also gave an energy correction formula that converges quadratically to the true eigenvalue. Various other propagators have also been used for the one-dimensional problem [14], but the Cooley algorithm suffices in most cases. However, it is worth mentioning the log-derivative propagators, which are important in many-channel problems, as will be seen below. The log-derivative methods rely on the fact that it is not actually necessary to propagate both the wavefunction and its derivative, since the normalisation of the wavefunction is arbitrary; it is adequate instead to propagate the logarithmic derivative $Y(R)$ of the wavefunction [14], defined by

$$Y(R) = \frac{d\chi}{dR}[\chi(R)]^{-1} = \frac{d \ln \chi}{dR}. \quad (8)$$

The condition for a trial energy to be an eigenvalue is then that the incoming and outgoing log-derivatives should be the same at the matching point. The log-derivative is a discontinuous function, with poles wherever $\chi(R)$ has nodes, so that some care is necessary in propagating it. Nevertheless, numerical methods are available [14,15,16] and are actually more stable than those for the wavefunction itself. Log-derivative methods are not widely used for the one-dimensional problem, but their greater numerical stability makes them the method of choice for many-channel problems.

2.2 Spectroscopic constants

The one-dimensional Schrödinger equation for an atom–atom Van der Waals molec-

ule has exactly the same form as for a normal chemically bound diatomic molecule. However, a Van der Waals molecule is typically much more weakly bound, and the intermolecular potential is capable of supporting only a few vibrational levels. The effects of anharmonicity and centrifugal distortion are much more pronounced than for most chemically bound species, and the representations necessary to describe the energy levels are somewhat different. In particular, the conventional expansion of diatomic energy levels in terms of Dunham coefficients Y_{ij} ,

$$E_{nl} = \sum_{ij} Y_{ij} (n + \frac{1}{2})^i [l(l + 1)]^j \quad (9)$$

is only slowly convergent for Van der Waals complexes. It is usually necessary to abandon the power series in $(n + \frac{1}{2})$, and to define a separate rotational expansion for each vibrational level,

$$E_{nl} = E_{n0} + B_n l(l + 1) - D_n [l(l + 1)]^2 + H_n [l(l + 1)]^3 + \dots \quad (10)$$

where B_n and D_n , H_n etc. are rotational and centrifugal distortion constants for vibrational level n . Efficient methods of calculating rotational and centrifugal distortion constants from the potential energy curve $V(R)$ are available [17]. If a very long progression in the rotational quantum number l is observed, the centrifugal distortion effects may be so large that even equation (10) is inadequate. Under these circumstances, it is necessary to solve equation (6) separately for each value of l .

For chemically bound diatomic molecules, it is usual to obtain the potential curve $V(R)$ by semiclassical (RKR) inversion [18,19] of (continuous) functions $G(n)$ and $B(n)$, which characterise the dependence of the vibrational energy and rotational constant on the vibrational quantum number n . This remains possible for Van der Waals complexes, although the procedure is hampered because there are usually relatively few vibrational levels, and this causes difficulty in interpolating $G(n)$ and $B(n)$. However, the shallow potential wells of Van der Waals complexes support only a limited number of rotational levels, and it is sometimes possible to follow E_{nl} for a particular vibrational level all the way to (centrifugal) dissociation. Child and Nesbitt [20] have proposed a variant of the RKR inversion procedure that allows a potential curve to be extracted from such data.

3. Atom–diatom Van der Waals molecules

When one of the atoms in an atom–atom Van der Waals molecule is replaced by a diatomic molecule, the dynamical problem is complicated in two ways. First, the Van der Waals complex may be formed from a diatom in any one of its vibration-rotation states, and each of these monomer states will give rise to a manifold of states of the complex. Secondly, the intermolecular potential for an atom–diatom system depends on the length of the diatom bond and on the relative orientation of the interacting species as well as on their separation. For complexes formed from diatomic molecules with electronic angular momentum the situation is even more complicated, but for simplicity

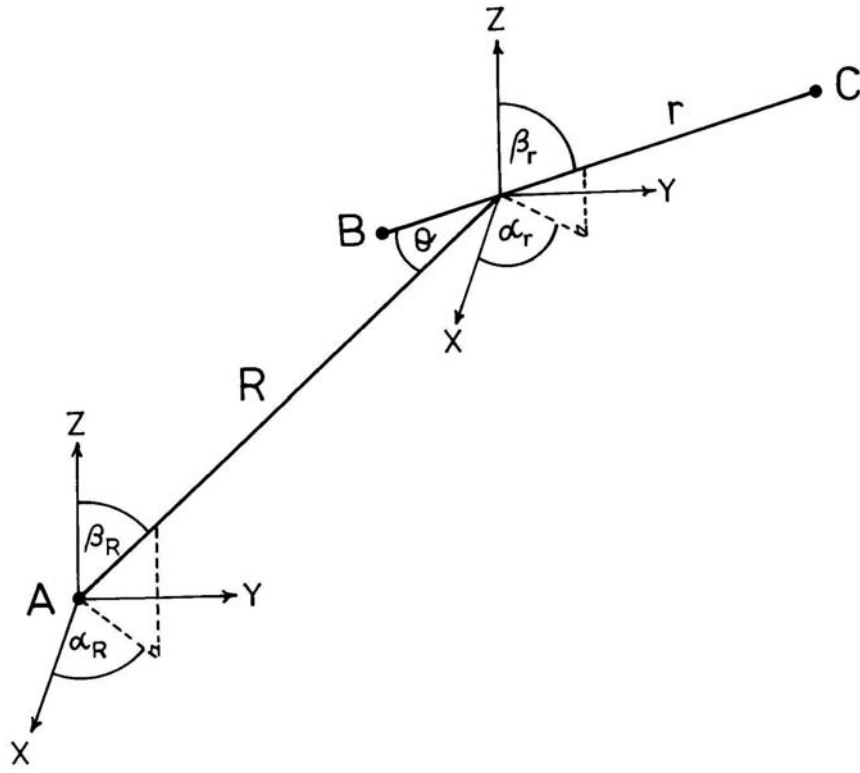


Figure 1. Coordinate system for atom–diatom Van der Waals complexes.

the treatment given below will be confined to Van der Waals molecules formed from closed-shell atoms and molecules.

An important feature of Van der Waals complexes is that the monomers involved retain their identity in the complex. It is thus desirable to choose a coordinate system and a form of the Hamiltonian that reflect this. Conventional normal mode Hamiltonians are generally not useful for Van der Waals complexes, because of the very wide amplitude and anharmonic character of the vibrational motions.

The coordinate system most commonly used for an atom–diatom Van der Waals complex is shown in Figure 1. The vector from the centre of mass of the diatom BC to the atom A is denoted \mathbf{R} , and has length R . The vector between the atoms B and C is \mathbf{r} , and is usually taken to originate on the heavier of atoms B and C. The length of \mathbf{r} is r , and the angle between \mathbf{R} and \mathbf{r} is θ . This is sometimes referred to as a Jacobi axis system. The unit vectors corresponding to \mathbf{R} and \mathbf{r} are denoted $\hat{\mathbf{R}}$ and $\hat{\mathbf{r}}$, and their orientations in a space-fixed axis system are described by the Euler angles (α_R, β_R) and (α_r, β_r) . The use of these unit vectors as function arguments will be used below as a shorthand for the angles defining their orientations: thus $Y_{lm}(\hat{\mathbf{R}}) \equiv Y_{lm}(\beta_R, \alpha_R)$ etc.

The Hamiltonian for an atom–diatom complex is a simple generalisation of the atom–atom Hamiltonian

$$H = -\frac{\hbar^2}{2\mu} R^{-1} \left(\frac{\partial^2}{\partial R^2} \right) R + \frac{\hbar^2 \hat{l}^2}{2\mu R^2} + V(R, r, \theta) + H_{\text{mon}}, \quad (11)$$

where μ is now $m_A m_{BC} / (m_A + m_{BC})$ and H_{mon} is the Hamiltonian for the isolated diatomic molecule BC. Unfortunately, the θ - and r -dependence of the intermolecular

potential destroys the separability of the Schrödinger equation, so that the dynamics of triatomic Van der Waals complexes are much more complicated than those of diatomic species.

3.1 Representation of the intermolecular potential

The intermolecular potential between an atom and a closed-shell diatomic molecule is a function of the three coordinates R , r and θ . When performing dynamical calculations, matrix elements of the potential are often required between angular-momentum eigenfunctions, and these matrix elements are greatly simplified if the potential is expanded in terms of Legendre polynomials

$$V(R, r, \theta) = \sum_{\lambda} V_{\lambda}(R, r) P_{\lambda}(\cos \theta) \quad (12)$$

where the functions $V_{\lambda}(R, r)$ are known as *radial strength functions*. This is a completely general representation, in that *any* potential function can be represented in this way if enough terms are included in the expansion.

Although equation (12) is completely general, it does not necessarily provide a compact parameterisation of the intermolecular potential, and other functional forms are often used instead. However, the Legendre expansion is readily obtained from any other representation by numerical quadrature. Because of the orthogonality property of the Legendre polynomials [21], equation (12) may be inverted to give

$$V_{\lambda}(R, r) = (\lambda + \frac{1}{2}) \int_0^{\pi} V(R, r, \theta) P_{\lambda}(\cos \theta) \sin \theta d\theta. \quad (13)$$

This integral may be simply evaluated numerically to any desired accuracy using Gaussian quadrature

$$V_{\lambda}(R, r) \approx (\lambda + \frac{1}{2}) \sum_{i=1}^N V(R, r, \arccos x_i) P_{\lambda}(x_i) w_i, \quad (14)$$

where the quantities x_i and w_i are points and weights for N -point Gauss-Legendre quadrature [21]. A minimum number of $(\lambda + 1)$ quadrature points is required to extract Legendre components up to $V_{\lambda}(R, r)$.

For Van der Waals molecules involving homonuclear diatomic molecules, the potential is symmetric about $\theta = \pi/2$,

$$V(R, r, \theta) = V(R, r, \pi - \theta). \quad (15)$$

This causes the integral of equation (13) to vanish for odd values of λ , so that for homonuclear diatoms the sum over λ in equation (12) is restricted to even values.

A further point of interest is the relationship between the intermolecular potentials for two different isotopic species of a Van der Waals molecule [22,23]. Within the electronic Born-Oppenheimer approximation, the intermolecular potential for a particular choice of the internuclear distances is independent of the nuclear masses. However, the coordinates R and θ are referred to the centre of mass of the diatomic molecule, and the position of this does depend on the nuclear masses involved. This affects the coefficients of the Legendre expansion of the intermolecular potential: for example, although the the potential for $\text{H}_2\text{-Ar}$ is symmetric about $\theta = \pi/2$ and thus includes only even-order Legendre terms, that for HD-Ar includes odd-order terms *when expanded about the centre of mass of HD*.

If the centre of mass shifts by a distance δ in the direction of r , the new coordinates (R, θ) corresponding to a particular nuclear geometry are related to the old coordinates (R', θ') by

$$R' = R(1 + t^2 + 2t \cos \theta)^{\frac{1}{2}}, \quad (16)$$

$$\cos \theta' = (\cos \theta + t)/(1 + t^2 + 2t \cos \theta)^{\frac{1}{2}}, \quad (17)$$

where $t = \delta/R$. Applying equation (13), the radial strength functions in the transformed coordinate system are

$$V_\lambda(R, r) = (\lambda + \frac{1}{2}) \int_0^\pi V(R', r, \theta') P_\lambda(\cos \theta) \sin \theta d\theta. \quad (18)$$

This integral may again be evaluated efficiently by Gaussian quadrature. It provides a method for obtaining the Legendre expansion of the potential energy surface for one Van der Waals molecule from the potential of an isotopically related system.

3.2 The coupled equations

A characteristic feature of Van der Waals molecules is that the intermolecular potential is sufficiently weak that the constituent molecules remain identifiable. It is thus natural to expand the wavefunction of the complex in terms of the vibration-rotation wavefunctions of the separated monomers, and a convenient expansion for atom-diatom systems is

$$\psi_\alpha(\mathbf{R}, \mathbf{r}) = r^{-1} R^{-1} \sum_{va} \phi_{vj}(r) \Phi_a(\hat{\mathbf{R}}, \hat{\mathbf{r}}) \chi_{va}^\alpha(R). \quad (19)$$

Here α labels a particular quantum state of the complex, $\phi_{vj}(r)$ is the stretching wavefunction of the free diatom with vibrational quantum number v and angular momentum j , and the functions $\Phi_a(\hat{\mathbf{R}}, \hat{\mathbf{r}})$ are a complete orthonormal set of *channel functions* spanning the space of the angular coordinates $\alpha_R, \beta_R, \alpha_r$ and β_r . The index a collectively labels the set of angular quantum numbers, including j . There are several possible choices for the channel functions, which will be discussed in detail below.

When this representation of the wavefunction is substituted into the total Schrödinger equation of the complex, using the Hamiltonian of equation (11), the equation

obtained is

$$\sum_{va} \left[-\frac{\hbar^2}{2\mu} R^{-1} \left(\frac{\partial^2}{\partial R^2} \right) R + \frac{\hbar^2 \hat{l}^2}{2\mu R^2} + V(R, r, \theta) + E_{vj}^{\text{mon}} - E \right] r^{-1} R^{-1} \phi_{vj}(r) \Phi_a(\hat{\mathbf{R}}, \hat{\mathbf{r}}) \chi_{va}^\alpha(R) = 0. \quad (20)$$

Multiplying this equation from the left by $\left[r^{-1} R^{-1} \phi_{v'j'}(r) \Phi_{a'}(\hat{\mathbf{R}}, \hat{\mathbf{r}}) \right]^*$ and integrating over all coordinates *except* R yields the *coupled equations* for the system

$$\begin{aligned} & \left[-\frac{\hbar^2}{2\mu} \frac{d^2}{dR^2} + (va|V|va) + (a| \frac{\hbar^2 \hat{l}^2}{2\mu R^2} |a) + E_{vj}^{\text{mon}} - E \right] \chi_{va}^\alpha(R) \\ & = - \sum'_{v'a'} \left[(va|V|v'a') + (a| \frac{\hbar^2 \hat{l}^2}{2\mu R^2} |a') \delta_{vv'} \right] \chi_{v'a'}^\alpha(R). \end{aligned} \quad (21)$$

This is a set of differential equations, one for each *channel* (labelled by va) included in the basis set. Terms off-diagonal in va , which couple the different equations, have been taken to the right hand side. The symbol \sum' indicates summation over all $v'a' \neq va$. The round bracket notation $(| |)$ has been adopted to indicate integration over all dynamical variables for which the associated quantum numbers are given; thus $(a|V|a')$ implies integration over the angular variables only, while $(va|V|v'a')$ implies an additional integral over the diatom stretching coordinate r .

The coupled equations are the most fundamental form of the Schrödinger equation for Van der Waals molecules, and most of the approximate methods described below can be derived by making simplifying approximations to the coupled equations. However, before proceeding further it is desirable to investigate the properties of the various channel basis sets which can be used in equation (19), and to describe the evaluation of the matrix elements involved in equation (21).

3.2.1 The space-fixed representation

There are two sources of angular momentum in an atom–diatom Van der Waals molecule: the end-over-end angular momentum of the complex l and the internal angular momentum of the diatom j . It would thus be possible to use as channel functions the simple products

$$\Phi_a(\hat{\mathbf{R}}, \hat{\mathbf{r}}) = Y_{jm_j}(\hat{\mathbf{r}}) Y_{lm_l}(\hat{\mathbf{R}}). \quad (22)$$

However, j and l couple together to form the total angular momentum J , which (in the absence of nuclear spin) is a rigorously good quantum number because of the isotropic nature of space. A more convenient choice of angular basis set is thus the set of simul-

taneous eigenfunctions of \hat{j}^2 , \hat{l}^2 , \hat{J}^2 and \hat{J}_Z

$$\begin{aligned}
\Phi_a(\hat{\mathbf{R}}, \hat{\mathbf{r}}) &\equiv \mathcal{Y}_{jl}^{JM}(\hat{\mathbf{R}}, \hat{\mathbf{r}}) \\
&= \sum_{m_j m_l} \langle j l m_j m_l | J M \rangle Y_{j m_j}(\hat{\mathbf{r}}) Y_{l m_l}(\hat{\mathbf{R}}) \\
&= \sum_{m_j m_l} (-)^{j-l+M} (2J+1)^{\frac{1}{2}} \begin{pmatrix} j & l & J \\ m_j & m_l & -M \end{pmatrix} Y_{j m_j}(\hat{\mathbf{r}}) Y_{l m_l}(\hat{\mathbf{R}}),
\end{aligned} \tag{23}$$

where $\langle j l m_j m_l | J M \rangle$ is a Clebsch-Gordan coefficient and $\begin{pmatrix} \cdot & \cdot & \cdot \\ \cdot & \cdot & \cdot \end{pmatrix}$ is a Wigner $3j$ -symbol [9]. Equation (19) with this choice of the $\Phi_a(\hat{\mathbf{R}}, \hat{\mathbf{r}})$ is known as the *space-fixed representation* of the wavefunction. For given values of j and l , J may take values from $|j-l|$ to $j+l$ in unit steps.

In order to calculate matrix elements of the total Hamiltonian between these angular functions, we need to know the effects of the operators H_{mon} and $V(\mathbf{R}, r, \theta)$. The space-fixed channel functions are eigenfunctions of H_{mon} when combined with the diatom stretching functions $\phi_{vj}(r)$

$$H_{\text{mon}} \left[r^{-1} \phi_{vj}(r) \Phi_a(\hat{\mathbf{R}}, \hat{\mathbf{r}}) \right] = E_{vj}^{\text{mon}} \left[r^{-1} \phi_{vj}(r) \Phi_a(\hat{\mathbf{R}}, \hat{\mathbf{r}}) \right], \tag{24}$$

where E_{vj}^{mon} is the energy of the isolated diatom in internal state (v, j) . H_{mon} thus has only diagonal matrix elements between the channel functions.

If the intermolecular potential is expanded in the form (12), its matrix elements may be expressed in terms of matrix elements of Legendre polynomials,

$$(v j l J | V | v' j' l' J) = \sum_{\lambda} f_{\lambda}(j l; j' l'; J) \int \phi_{vj}(r) V_{\lambda}(\mathbf{R}, r) \phi_{v'j'}(r) dr, \tag{25}$$

where the Percival-Seaton coefficients $f_{\lambda}(j l; j' l'; J)$ are

$$\begin{aligned}
f_{\lambda}(j l; j' l'; J) &= (j l J M | P_{\lambda}(\cos \theta) | j' l' J M) \\
&= (-)^{l+l'+J} [(2j+1)(2j'+1)(2l+1)(2l'+1)]^{\frac{1}{2}} \\
&\times \begin{pmatrix} l & \lambda & l' \\ 0 & 0 & 0 \end{pmatrix} \begin{pmatrix} j & \lambda & j' \\ 0 & 0 & 0 \end{pmatrix} \left\{ \begin{matrix} l & \lambda & l' \\ j' & J & j \end{matrix} \right\},
\end{aligned} \tag{26}$$

and $\left\{ \begin{matrix} \cdot & \cdot & \cdot \\ \cdot & \cdot & \cdot \end{matrix} \right\}$ is a Wigner $6j$ -symbol [9]. The potential matrix elements off-diagonal in v have only a very small effect on bound state energy levels, but are crucial in calculations of vibrational predissociation or vibrational relaxation rates. Because of the presence of the two $3j$ -symbols with vanishing projection quantum numbers, the Percival-Seaton coefficients are zero unless

- 1) Triangle relationships are satisfied by (j, λ, j') and (l, λ, l')
- 2) Both $(j + \lambda + j')$ and $(l + \lambda + l')$ are even.

These restrictions have important consequences for the diagonal matrix elements of the intermolecular potential. In particular,

- 1) Only Legendre components with $\lambda \leq 2j$ can contribute to the diagonal potential for a given channel.
- 2) Odd-order Legendre terms have no matrix elements diagonal in j .

The Percival-Seaton coefficients are diagonal in both J and the *parity* $p' = (-)^{j+l}$. The intermolecular potential cannot mix states of different J or p' , and these are rigorously good quantum numbers for a Van der Waals molecule. *

In the space-fixed representation, the coupled equations are thus

$$\left[-\frac{\hbar^2}{2\mu} \frac{d^2}{dR^2} + (vjlJ|V|vjlJ) + \frac{\hbar^2 l(l+1)}{2\mu R^2} + E_{vj}^{\text{mon}} - E \right] \chi_{jlJ}^J(R) = - \sum'_{v'j'l'} (vjlJ|V|v'j'l'J) \chi_{v'j'l'}^J(R). \quad (27)$$

3.2.2 The body-fixed representation

The space-fixed basis set described in the previous section provides a representation in which the end-over-end angular momentum operator \hat{l}^2 is diagonal, and channels of different l and j are coupled by the intermolecular potential. This is appropriate when the anisotropy of the intermolecular potential is weak, but for strongly anisotropic systems it is often more convenient to use a *body-fixed* (or *molecule-fixed*) basis set, in which the intermolecular potential is block-diagonal, and most of the coupling between channels comes from the \hat{l}^2 operator.

In order to obtain the body-fixed representation, the Hamiltonian is first transformed to a coordinate system that rotates with the complex, rather than being fixed in space. The orientation of the body-fixed axes (x, y, z) relative to the space-fixed axes (X, Y, Z) is described by the Euler angles $(\alpha, \beta, 0)$, where $(\beta, \alpha) \equiv (\beta_R, \alpha_R)$ are the polar coordinates of the \mathbf{R} vector in the space-fixed axis system. The polar and azimuthal angles of the \mathbf{r} vector in the body-fixed axis system are denoted θ and ϕ . This coordinate system has been termed the “two-thirds body-fixed” system [24], since only two of the three Euler angles are used in specifying the orientation of the body-fixed axes.

* A slightly different quantity, $p = (-)^{j+l+J}$, is used in much of the scattering literature. This too is sometimes referred to as parity, and is a rigorously good quantum number, but is sometimes less convenient than p' when formulating spectroscopic selection rules. In spectroscopic terms, states with $p = +1$ and -1 are often labelled e and f respectively.

The Hamiltonian obtained directly on transforming to the body-fixed system is inconvenient to use, since the commutation properties of the angular momenta involved are very complicated [24]. However, it is possible to define an *isomorphic* Hamiltonian where the commutation properties are simpler [25,26]. The isomorphic Hamiltonian is related to the true Hamiltonian by

$$H_{\text{iso}} = U H U^{-1}, \quad (28)$$

where

$$U = \exp(i\phi' \hat{j}_z) \quad (29)$$

and ϕ' is an artificial independent variable not present in the true Hamiltonian. The isomorphic Hamiltonian has the same eigenvalues as the true Hamiltonian [26], and may be written in the form

$$H_{\text{iso}} = -\frac{\hbar^2}{2\mu} R^{-1} \left(\frac{\partial^2}{\partial R^2} \right) R + \frac{\hbar^2 (\hat{J} - \hat{j})^2}{2\mu R^2} + V(R, r, \theta) + H_{\text{mon}}, \quad (30)$$

Here, \hat{J} is the operator for the total angular momentum, evaluated in the space-fixed axis system and projected onto the body-fixed frame defined by the angles (α, β, ϕ') , and \hat{j} is the body-fixed angular momentum operator for the diatomic molecule. Since the isomorphic Hamiltonian involves one more angular coordinate than the true Hamiltonian, its eigenfunctions are characterised by an extra body-fixed projection quantum number. The eigenfunctions may be expanded in the angular basis set

$$\left(\frac{2J+1}{8\pi^2} \right)^{\frac{1}{2}} \mathcal{D}_{MK}^{J*}(\alpha, \beta, \phi') Y_{jk}(\theta, \phi), \quad (31)$$

where $\mathcal{D}_{MK}^J(\alpha, \beta, \phi')$ is a rotation matrix element with the phase convention of Brink and Satchler [9] and $Y_{jk}(\theta, \phi)$ is a spherical harmonic involving the angular coordinates of the diatomic molecule in the body-fixed axis system.

Physically, the end-over-end angular momentum of the complex cannot have any body-fixed projection along \mathbf{R} , so that the projection of \mathbf{J} onto the \mathbf{R} vector must be the same as the projection of \mathbf{j} . The physically significant eigenfunctions of the isomorphic Hamiltonian are thus those with $K = k$, and the basis set appropriate for expanding the eigenfunctions of the true Hamiltonian is

$$\begin{aligned} \Phi_{jK}^{JM}(\hat{\mathbf{R}}, \hat{\mathbf{r}}) &= (2\pi)^{\frac{1}{2}} U^{-1} \left(\frac{2J+1}{8\pi^2} \right)^{\frac{1}{2}} \mathcal{D}_{MK}^{J*}(\alpha, \beta, \phi') Y_{jK}(\theta, \phi) \\ &= \left(\frac{2J+1}{4\pi} \right)^{\frac{1}{2}} \mathcal{D}_{MK}^{J*}(\alpha, \beta, 0) Y_{jK}(\theta, \phi). \end{aligned} \quad (32)$$

The artificial angle has thus disappeared in the basis functions for the true Hamiltonian, as required.

The matrix elements of the intermolecular potential are particularly simple in the body-fixed representation, and are diagonal in both J and K . They are given by

$$(jKJM|P_\lambda(\cos\theta)|j'K'JM) = \delta_{KK'}g_\lambda(jj'K), \quad (33)$$

where

$$g_\lambda(jj'K) = (-)^K [(2j+1)(2j'+1)]^{\frac{1}{2}} \begin{pmatrix} j & \lambda & j' \\ 0 & 0 & 0 \end{pmatrix} \begin{pmatrix} j & \lambda & j' \\ -K & 0 & K \end{pmatrix}. \quad (34)$$

The potential matrix elements are thus independent of J , unlike those of the space-fixed representation. The presence of the first $3j$ -symbol in this equation again ensures that the matrix elements vanish unless $(j + \lambda + j')$ is even and (j, λ, j') satisfy a triangle relationship.

The matrix elements of the operator $(\hat{J} - \hat{j})^2$ may be obtained by expanding it as follows

$$\begin{aligned} (\hat{J} - \hat{j})^2 &= \hat{J}^2 + \hat{j}^2 - 2\hat{j} \cdot \hat{J} \\ &= \hat{J}^2 + \hat{j}^2 - 2\hat{j}_z \hat{J}_z - 2\hat{j}_x \hat{J}_x - 2\hat{j}_y \hat{J}_y \\ &= \hat{J}^2 + \hat{j}^2 - 2\hat{J}_z^2 - \hat{j}_- \hat{J}_- - \hat{j}_+ \hat{J}_+ \end{aligned} \quad (35)$$

where

$$\hat{J}_\pm = \hat{J}_x \mp i\hat{J}_y \quad (36)$$

and

$$\hat{j}_\pm = \hat{j}_x \pm i\hat{j}_y \quad (37)$$

are raising and lowering operators in the body-fixed axis system, and the equivalence of the operators \hat{J}_z and \hat{j}_z has been used. Note the inverted sign in the definition of \hat{J}_\pm , which arises because the components of \hat{J} referred to body-fixed axes obey ‘‘anomalous’’ commutation relationships [27].

The matrix elements of $(\hat{J} - \hat{j})^2$ are thus

$$\begin{aligned} \langle jKJM|(\hat{J} - \hat{j})^2|jKJM\rangle &= J(J+1) + j(j+1) - 2K^2 \\ \langle jKJM|(\hat{J} - \hat{j})^2|jK \pm 1JM\rangle &= [J(J+1) - K(K \pm 1)]^{\frac{1}{2}} [j(j+1) - K(K \pm 1)]^{\frac{1}{2}} \\ &= c(j; KK \pm 1; J), \end{aligned} \quad (38)$$

with all other matrix elements zero.

In the body-fixed representation, the coupled equations are thus

$$\begin{aligned}
& \left[-\frac{\hbar^2}{2\mu} \frac{d^2}{dR^2} + (vjKJ|V|vjKJ) \right. \\
& \quad \left. + \frac{\hbar^2}{2\mu R^2} [J(J+1) + j(j+1) - 2K^2] + E_{vj}^{\text{mon}} - E \right] \chi_{vjK}^J(R) \\
& = - \sum'_{v'j'} (vjKJ|V|v'j'KJ) \chi_{v'j'K}^J(R) \\
& \quad + \sum'_{K'=K\pm 1} \frac{\hbar^2}{2\mu R^2} c(j; KK'; J) \chi_{vjK'}^J(R),
\end{aligned} \tag{39}$$

where

$$(vjKJ|V|v'j'KJ) = \sum_{\lambda} g_{\lambda}(jj'K) \int \phi_{vj}(r) V_{\lambda}(R, r) \phi_{v'j'}(r) dr. \tag{40}$$

The primitive body-fixed basis functions as described above do not have definite parity, except for $K = 0$. However, since parity is a rigorously good quantum number, it is usually advantageous to choose basis functions that do have definite parity, and it is straightforward to define linear combinations of the primitive functions for which this is the case. Adopting the notation $\Omega \equiv |K|$, these are

$$\Phi_{j\Omega}^{JM\pm}(\hat{\mathbf{R}}, \hat{\mathbf{r}}) = N \left[\mathcal{D}_{M\Omega}^{J*}(\alpha, \beta, 0) Y_{j\Omega}(\theta, \phi) \pm (-)^J \mathcal{D}_{M-\Omega}^{J*}(\alpha, \beta, 0) Y_{j-\Omega}(\theta, \phi) \right], \tag{41}$$

where the normalising factor N is $[(2J+1)/16\pi]^{\frac{1}{2}}$ for $\Omega = 0$ and $[(2J+1)/8\pi]^{\frac{1}{2}}$ for $\Omega > 0$. These basis functions are referred to as the *parity-adapted* body-fixed basis set; the matrix elements of the Van der Waals Hamiltonian between these functions are readily constructed from the matrix elements between the primitive body-fixed functions.

3.2.3 Transformation between space-fixed and body-fixed representations

The space-fixed and body-fixed basis sets both span the space of the angular coordinates $\alpha_R, \beta_R, \alpha_r$ and β_r , and are related by the expressions

$$\begin{aligned}
\mathcal{Y}_{jl}^{JM}(\hat{\mathbf{R}}, \hat{\mathbf{r}}) & = \sum_K \mathcal{D}_{MK}^{J*}(\alpha, \beta, 0) \langle jlK0|JK \rangle Y_{jK}(\theta, \phi) Y_{l0}(0, 0) \\
& = (2l+1)^{\frac{1}{2}} \sum_K (-)^{j-l-K} \begin{pmatrix} j & l & J \\ K & 0 & -K \end{pmatrix} \Phi_{jK}^{JM}(\hat{\mathbf{R}}, \hat{\mathbf{r}})
\end{aligned} \tag{42}$$

and conversely

$$\Phi_{jK}^{JM}(\hat{\mathbf{R}}, \hat{\mathbf{r}}) = \sum_l (-)^{j-l-K} (2l+1)^{\frac{1}{2}} \begin{pmatrix} j & l & J \\ K & 0 & -K \end{pmatrix} \mathcal{Y}_{jl}^{JM}(\hat{\mathbf{R}}, \hat{\mathbf{r}}). \tag{43}$$

These equations have several important consequences:

- 1) The j quantum number is unaffected by the transformation. Thus, a space-fixed basis set which includes all l values corresponding to a particular J and j spans exactly the same space as a body-fixed basis set which contains all values of K for that J and j . If the coupled equations are solved exactly, there is no difference between the solutions obtained in the space-fixed and body-fixed representations.
- 2) If $J = 0$ or $j = 0$, the summations on the right hand sides of equations (42) and (43) collapse to a single term. Under these circumstances, there is no difference between the space-fixed and body-fixed representations. This is also true for the even parity ($p' = +1$, f symmetry) case with $J = 1$.

3.2.4 Solving the coupled equations

The coupled equations (27) and (39) take the general matrix form

$$\frac{d^2\chi}{dR^2} = [W(R) - \epsilon]\chi(R). \quad (44)$$

There are in principle an infinite number of channels (basis functions); it is usual to truncate the set to include only those channels which lie reasonably close in energy to the state(s) of interest. This is known as the *close-coupling approximation*, and calculations which make no other dynamical approximation are known as *close-coupling calculations* to distinguish them from the various decoupling approximations discussed below. If N channels are included in the expansion, $W(R)$ is an $N \times N$ matrix and $\epsilon = (2\mu E/\hbar^2)I$ is a constant times the unit matrix. The physically significant bound state wavefunction $\chi(R)$, satisfying the boundary conditions at both $R = 0$ and $R = \infty$, is represented as a column vector with N components. However, if the boundary conditions are neglected, there are N linearly independent solution vectors at each energy, so that until the boundary conditions are applied it is actually necessary to propagate an $N \times N$ wavefunction matrix.

These equations are exactly the same as the coupled equations of molecular scattering theory, except that the boundary conditions are different for the bound state case. There are solutions of the coupled equations satisfying scattering boundary conditions for any energy greater than the dissociation energy of the complex, so that the scattering problem reduces to propagating solutions of the coupled equations from one value of R to another for a specified energy E . Many methods of doing this have been developed [15,16,28-33], but they are adequately treated in the scattering literature and are outside the scope of this article.

The additional problem present in the bound state case, at energies below the dissociation energy of the complex, is that of locating energies which are eigenvalues of the coupled equations, where a solution may be found that satisfies bound state boundary conditions: for bound states, each component of χ must satisfy equation (7). There are several procedures available for doing this [34-37]. The earliest, due to Dunker and Gordon [34], is a straightforward extension of the shooting procedure used in the

one-dimensional case: incoming and outgoing solutions of the coupled equations are started in the short-range and long-range classically forbidden regions, and matched in the classically allowed region, allowing an initial estimate of the eigenvalue to be refined iteratively. Dunker and Gordon have given an explicit generalisation of the matching criterion, involving both the wavefunction matrix and its derivative. However, as is well known in scattering theory, wavefunction propagation methods are subject to a classic numerical instability, which is particularly serious for bound-state problems because it is usually necessary to include many closed channels in the calculations. The wavefunction component $\chi_i(R)$ for a locally open channel i (with $W_{ii}(R) < \epsilon$) is an oscillatory function of R , whereas that for a locally closed channel (with $W_{ii}(R) > \epsilon$) is made up of exponentially increasing and decreasing components. If there are both locally open and locally closed channels over any range of R , there is a tendency for the closed channel components to grow so quickly that (because of numerical rounding errors) the linear independence of the different solutions is lost.

This problem is neatly circumvented by log-derivative methods. In the many-channel case, the log-derivative matrix $Y(R)$ is defined by [15]

$$Y(R) = \chi'(R)[\chi(R)]^{-1}, \quad (45)$$

where $\chi(R)$ is the $N \times N$ wavefunction matrix and the prime indicates radial differentiation. The diagonal elements of the log-derivative matrix become constant when $\chi(R)$ is exponentially increasing or decreasing, so that loss of linear independence does not occur. In addition, as foreshadowed in the discussion of the single-channel case above, the log-derivative matrix contains exactly the information needed to locate eigenvalues. As before, incoming and outgoing solutions are propagated from the two classically forbidden regions to a matching point in the classically allowed region: at an eigenvalue, the determinant of the difference between the two solutions is zero,

$$|Y^{\text{in}}(R_{\text{mid}}) - Y^{\text{out}}(R_{\text{mid}})| = 0. \quad (46)$$

The strategy to be adopted in searching for the zeroes of the matching determinant has been discussed in detail by Johnson [35] and Manolopoulos [16].

One apparent disadvantage of the log-derivative methods is that they do not directly give explicit wavefunctions, which are needed to calculate molecular properties (via expectation values) and spectroscopic intensities (via off-diagonal matrix elements). However, the restriction is not as serious as it might appear: a finite-difference approach for extracting expectation values from coupled channel calculations has been described by Hutson [38].

3.2.5 Matrix methods

An alternative approach to solving the coupled equations is to use a basis set expansion for the R coordinate as well as for r and the angular variables. The angular basis sets used in such calculations are generally the same as in coupled channel calculations.

This approach was pioneered for Van der Waals molecules by Le Roy and Van Kranendonk [39], who used numerical basis sets for the radial (R) functions. Such basis sets are adequate for the rare gas–H₂ systems, but converge very poorly for more strongly anisotropic systems. An alternative basis set, based on Morse-oscillator-like functions, has been used extensively by Tennyson and coworkers [10,40].

A recent development in this area has been the use of non-orthogonal basis sets of Gaussian functions (“distributed Gaussians”) [11]. These circumvent the problem of representing non-oscillatory regions of the wavefunction in terms of oscillatory functions, which is the major source of poor convergence in other types of basis-set calculation. They have been applied to simulating the spectra of a range of rare gas – hydrogen halide Van der Waals complexes by Clary and Nesbitt [41]. A particularly promising approach is the combination of distributed Gaussian basis sets (DGB) for the R motion with a discrete variable representation (DVR) for the angular motion [42].

4. Approximate methods

Although it is possible to solve the Schrödinger equation exactly for a particular potential surface, as described in the previous section, the computer time required is often substantial, and physical insight may be lost because of the complexity of the calculation. It is often more helpful to attempt an approximate factorisation of the wavefunction into components recognizable as vibrations or rotations of a particular part of the molecular framework. Calculations based on such approximations can offer considerable savings in computer time, and also preserve the physics of the problem in a more transparent form.

There is no single factorisation scheme that works well for all Van der Waals molecules. However, most of the commonly used schemes make a basic separation into three types of motion

- (1) Vibrations of individual monomers
- (2) The stretching vibration of the Van der Waals bond
- (3) Angular motions, including internal rotations, bending vibrations of the Van der Waals bond, and overall rotation of the complex.

The total energy is thus given approximately by

$$E^{\text{tot}} = E_{vj}^{\text{mon}} + E_n^{\text{stretch}} + E_a^{\text{ang}}. \quad (47)$$

The vibrational motions (1) and (2) are easily visualised and the energy contributions from them are simple. To a first approximation, E_{vj}^{mon} is just the energy that the monomers would have if isolated, and E_n^{stretch} is an eigenvalue of an effective one-dimensional potential, as discussed in section 4.3 below. The angular motions, however, are much more complex, and further factorisations are usually attempted; the following section will be devoted to the various separations which can be used. It is very important to choose the coupling scheme appropriate to the particular molecule of interest when performing approximate calculations.

4.1 Angular momentum coupling cases

There are several ways in which the angular momenta in a Van der Waals molecule may couple together, as pointed out by Bratoz and Martin [43], and the different coupling schemes give rise to qualitatively different patterns of energy levels. The coupling cases are most readily appreciated by considering a simplified model problem in which coupling between the angular $(\alpha_R, \beta_R, \alpha_r, \beta_r)$ and radial (R, r) motions is neglected. The Schrödinger equation for the angular motion is then

$$\left[b\hat{j}^2 + B\hat{l}^2 + V(\theta) - E \right] \Phi_\alpha^J(\hat{\mathbf{R}}, \hat{\mathbf{r}}) = 0, \quad (48)$$

where B and b are the rotational constants of the complex and of the diatomic molecule,

$$\begin{aligned} B &= \frac{\hbar^2}{2\mu} \langle R^{-2} \rangle, \\ b &= \frac{\hbar^2}{2\mu_{\text{mon}}} \langle r^{-2} \rangle, \end{aligned} \quad (49)$$

and $V(\theta)$ is the expectation value of $V(R, r, \theta)$ over the radial motions

$$\begin{aligned} V(\theta) &= \langle V(R, r, \theta) \rangle \\ &= \sum_{\lambda} V_{\lambda} P_{\lambda}(\cos \theta). \end{aligned} \quad (50)$$

The isotropic potential term, V_0 , merely shifts all the levels of the complex by a constant amount relative to the levels of the free diatom; the anisotropic terms V_1, V_2 etc. cause additional shifts and splittings of the observed levels.

It is usually true for Van der Waals molecules that $B \ll b$, since $\mu > \mu_{\text{mon}}$ and $R > r$. Denoting the dominant anisotropic term by V_{aniso} , three major coupling schemes can occur, depending on the relative magnitudes of B, b and V_{aniso} . These will be referred to here as coupling cases 1, 2 and 3 in order of increasing anisotropy; the coupling cases followed by various Van der Waals molecules in their lower energy states are given in Table 1, although it should be appreciated that the coupling case observed can be different for different internal states of the same Van der Waals molecule. *

4.1.1 Case 1

For small anisotropies, even-order Legendre terms in the potential are much more important than odd-order terms because only the former have diagonal matrix elements. For very small anisotropies, $V_2 < B$ (and consequently $V_2 \ll b$), the space-fixed representation of section 3.2.1 is appropriate. Both j and l are nearly good quantum numbers,

* The coupling cases referred to here as cases 1, 2 and 3 correspond to Bratoz and Martin's cases a, b and c. Their notation has been modified here to avoid confusion with Hund's coupling cases for diatomic molecules.

Table 1. Van der Waals complexes exhibiting different angular momentum coupling cases.

Case 1	Case 2*	Case 3
Rg-H ₂	Rg-HF	Rg-I ₂
Rg-HD	Rg-HCl	Rg-N ₂
Rg-D ₂	Rg-HBr	Rg-CO
		Rg-OCS

* These complexes exhibit case 2 coupling in states of low angular momentum. For higher angular momenta, a transition to case 1 is expected.

and couple together to form J . In a vector model, j and l may be considered to be precessing around the direction of J , as shown in Figure 2a, so that m_j and m_l are not individually conserved.

Pure case 1 coupling occurs only in the limit of zero anisotropy. For small anisotropies, however, the energy levels of the complex may be obtained from perturbation theory in the space-fixed basis set. To first order,

$$E_{jln}^J = E_{vj}^{\text{mon}} + E_n^{\text{stretch}} + Bl(l+1) + \sum_{\lambda} V_{\lambda} \langle jlJM | P_{\lambda}(\cos \theta) | jlJM \rangle. \quad (51)$$

The potential matrix elements are simply Percival-Seaton coefficients, equation (26), so that the angular factors in the diagonal matrix elements are zero unless λ is even. Neglecting V_4 and higher order terms, which are usually much smaller than V_2 , and substituting the diatomic rigid-rotor value for E_{vj}^{mon} , the energy expression becomes

$$E_{jln}^J = bj(j+1) + E_n^{\text{stretch}} + Bl(l+1) + V_0 + V_2 f_2(jl; jl; J). \quad (52)$$

Thus for atom-diatom complexes exhibiting case 1 coupling, there are groups of energy levels with a particular j , l and n , split by the V_2 anisotropy into components of different J . For each j and l , J can take all integer values from $|j-l|$ to $j+l$.

The classic systems exhibiting case 1 coupling are the rare gas-H₂ complexes, for which the anisotropy is quite small and B is relatively large. However, even for these systems the first-order treatment is only qualitatively valid, and it is necessary to consider off-diagonal potential terms. Second-order perturbation theory is reasonably accurate for these systems [39] although more sophisticated calculations are usually used [44].

Case 1 coupling begins to break down when perturbation theory in a space-fixed basis set is no longer adequate to treat the effects of anisotropy. The nearest level that can be coupled to $|jlJM\rangle$ by an anisotropic potential is $|jl-2JM\rangle$; the zeroth order energy separation between these levels is $(4l-2)B$. Case 1 coupling is thus appropriate if

$$V_2 f_2(jl; jl-2; J) \ll 4Bl. \quad (53)$$

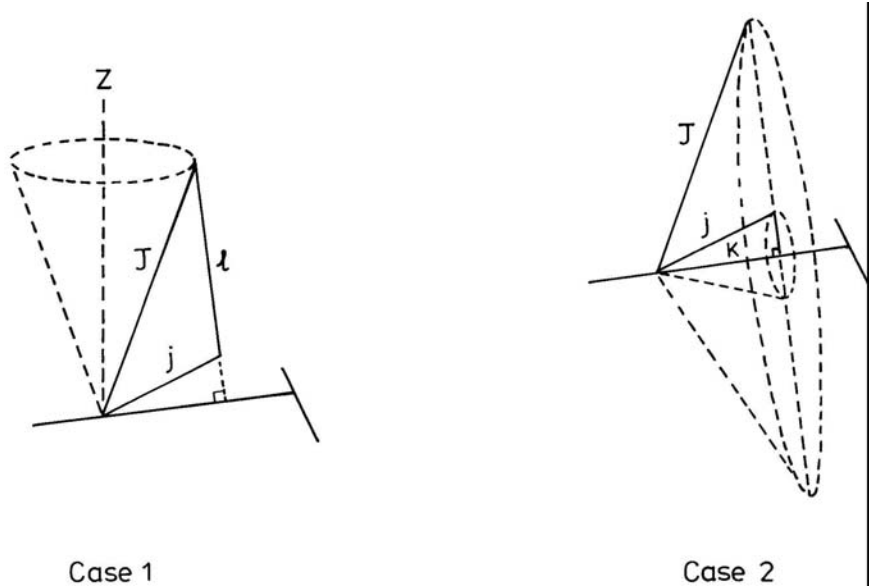


Figure 2. Angular momentum coupling cases.

This is a quantitative criterion for the applicability of case 1 coupling; it has the interesting consequence that case 1 coupling should be valid for all Van der Waals molecules at sufficiently high values of l (and J).

4.1.2 Case 2

Case 2 coupling occurs when the anisotropic potential terms are large compared to the separation of levels of different l for a particular j and J , but are still small compared to the separation between levels of different j . The end-over-end angular momentum l is no longer even nearly conserved, but j is still nearly a good quantum number. In a vector model, j is strongly coupled to the intermolecular axis R , with a projection K . K then couples to the end-over-end rotation of the complex to form J , as shown in Figure 2b.

Under case 2 conditions, the energy levels may be obtained approximately from a first-order perturbation treatment in the body-fixed basis set of section 3.2.2,

$$E_{jKn}^J = E_{vj}^{\text{mon}} + E_n^{\text{stretch}} + B[J(J+1) + j(j+1) - 2K^2] + \sum_{\lambda} V_{\lambda} \langle jKn | P_{\lambda}(\cos \theta) | jKn \rangle. \quad (54)$$

Once again there are no diagonal matrix elements of odd-order Legendre terms, and the first-order energy level expression neglecting high-order anisotropies is

$$E_{jKn}^J = bj(j+1) + E_n^{\text{stretch}} + B[J(J+1) + j(j+1) - 2K^2] + V_0 + V_2 g_2(jjK), \quad (55)$$

where $g_2(jjK)$ is defined by equation (34) above. However, since V_2 must be substantial for case 2 coupling to occur at all, it is nearly always necessary in accurate calculations to include higher-order effects due to potential terms off-diagonal in j (but diagonal in K).

In case 2 coupling, therefore, each monomer rotational level is split into groups of levels with $K = 0, \pm 1, \pm 2, \dots \pm j$. Within each (j, K) manifold, J can take any value $J \geq |K|$, and the resulting energy levels follow a diatomic-molecule-like energy expression

$$E_{jKn}^J = E_{jKn}^{(0)} + BJ(J+1). \quad (56)$$

However, it may be noted that the pattern of energy levels $E_{jKn}^{(0)}$ for different values of K is *not* that appropriate to a symmetric top. The splittings between the different K levels contain important contributions from the potential energy terms $V_2 g_2(jjK)$, in addition to those arising from the rotational kinetic energy.

For real Van der Waals molecules, it is necessary to go beyond the case 2 limit and consider the neglected Coriolis terms arising from $B(\hat{J} - \hat{j})^2$ in second order. In the case 2 basis set, the matrix elements of $(\hat{J} - \hat{j})^2$ are given by equation (38). They connect states of the *same* J , j and parity, with Ω differing by ± 1 . The matrix elements are the same for (+) and (-) parities, except that only $(-)^J$ (e) parity states exist for $\Omega = 0$. Their effect is to resolve the degeneracy between (+) and (-) parity states for $\Omega > 0$; the energy splitting is greatest for $\Omega = 1$ states, because the $(-)^J$ (e) parity levels are shifted by coupling to the corresponding $\Omega = 0$ state, and the $(-)^{J+1}$ (f) parity states are not. The effect of Coriolis coupling on an Ω -state first appears in the 2Ω th order of perturbation theory.

The Coriolis matrix elements increase substantially with increasing j and J . For small Coriolis matrix elements and well-separated case 2 states, it may be adequate to treat the Coriolis coupling by second-order perturbation theory. Under these circumstances, their effect on the spectrum is simply to introduce different rotational constants for e and f levels. The difference is usually only important for Π ($\Omega = 1$) states, and is characterised by an l -type doubling constant q_l , such that

$$\begin{aligned} B_f &= B + \frac{1}{2}q_l = \frac{\hbar^2}{2\mu} \langle R^{-2} \rangle \\ B_e &= B - \frac{1}{2}q_l = \frac{\hbar^2}{2\mu} \langle R^{-2} \rangle - q_l \end{aligned} \quad (57)$$

However, for sufficiently large J and j the perturbation treatment always breaks down. Under these circumstances it is necessary to construct and diagonalise a (small) Hamiltonian matrix directly, as described by Lovejoy and Nesbitt [45] in the case of Ar-HCl.

The range of validity of case 2 coupling is limited by the requirement that the off-diagonal matrix elements be small compared to the separation of the energy levels involved. Since the Coriolis matrix elements couple levels with $\Delta K = \pm 1$, this requirement becomes

$$B[j(j+1) - K(K \pm 1)]^{\frac{1}{2}} [J(J+1) - K(K \pm 1)]^{\frac{1}{2}} \ll V_2 [g_2(jjK \pm 1) - g_2(jjK)]. \quad (58)$$

This condition is complementary to equation (53); case 2 coupling takes over from case 1 coupling as the V_2 anisotropy is increased or the angular momentum quantum numbers decrease. This changeover will be described in more detail below, but it is important to note here that odd-order anisotropies (in particular, V_1) play very little role in the changeover from case 1 to case 2.

Case 2 coupling may also break down if the anisotropy is high enough to cause significant mixing of states of different j . This will occur if

$$\begin{aligned} & V_1 g_1(j, j-1, K) \approx 2bj \\ \text{or} & \quad V_2 g_2(j, j-2, K) \approx 4bj \quad \text{etc.} \end{aligned} \tag{59}$$

and under these circumstances case 3 coupling takes over as discussed below. Since the potential matrix elements involved here are no longer diagonal in j , odd-order anisotropies can be effective in causing the changeover from case 2 to case 3 coupling. In contrast to the 1–2 changeover, the 2–3 changeover is not affected by the degree of rotational (J) excitation of the complex, since neither the potential matrix elements nor the separation between levels of different j depend on the total angular momentum J . However, since j is no longer a good quantum number in case 3, there can be Coriolis matrix elements between states that are nominally labelled by different j values.

4.1.3 Case 3

Case 3 coupling occurs when the potential anisotropy is large compared to the rotational constant of the diatom b , so that the complex is a nearly rigid molecule executing torsional oscillations about its equilibrium geometry. Under these conditions, neither j nor l is a good quantum number, but K is still nearly conserved. The vector model for case 3 is similar to that for case 2, except that only the projection of j onto R is well-defined, not j itself.

The choice of a basis set for a case 3 Van der Waals molecule is more difficult than for cases 1 and 2. It is still often feasible to expand the wavefunction in a body-fixed (case 2) basis set, although it may be necessary to include many j levels to obtain convergence. Alternatively, and more appropriately, a basis set of vibrational functions centred on the equilibrium geometry may be used. The basis sets that are appropriate are different for linear and non-linear equilibrium geometries.

For a linear equilibrium geometry, the angular Hamiltonian may be approximated around $\theta = 0$,

$$\begin{aligned} H &= b\hat{j}^2 + V(\theta) \\ &= -\frac{b}{\sin^2 \theta} \left[\sin \theta \frac{\partial}{\partial \theta} \left(\sin \theta \frac{\partial}{\partial \theta} \right) + \frac{\partial^2}{\partial \alpha^2} \right] + V(\theta) \\ &\approx -b \left[\frac{1}{\theta} \frac{\partial}{\partial \theta} + \frac{\partial^2}{\partial \theta^2} + \frac{1}{\theta^2} \frac{\partial^2}{\partial \alpha^2} \right] + V(\theta). \end{aligned} \tag{60}$$

The quantity in brackets in the last line is just the two-dimensional Laplacian in polar coordinates; transforming to Cartesian coordinates defined by

$$\begin{aligned}x &= \sin \theta \cos \alpha \\y &= \sin \theta \sin \alpha,\end{aligned}\tag{61}$$

the Hamiltonian becomes

$$H = -b \left[\frac{\partial^2}{\partial x^2} + \frac{\partial^2}{\partial y^2} \right] + V(\theta).\tag{62}$$

Since the potential has cylindrical symmetry, it may be written as a function of ρ , where

$$\begin{aligned}\rho^2 &= x^2 + y^2 = \sin^2 \theta \\V(\theta) &= V'(\rho) = V_0 + V_2 \rho^2 + V_4 \rho^4 + \dots\end{aligned}\tag{63}$$

Note that the coefficient V_2 does not have the same meaning here as in the earlier discussion. The eigenvalues of a linear case 3 complex are thus those of a symmetric two-dimensional oscillator. If the complex is sufficiently anisotropic that only the quadratic potential term in equation (63) is significant in the classically allowed region, the levels are those of a two-dimensional harmonic oscillator

$$E_{vK}^{\text{ang}} = V_0 + 2\sqrt{V_2 b} \left(v + \frac{1}{2} \right).\tag{64}$$

In this limit, the bending vibrational levels are equally spaced, with the v th level having a degeneracy of $(v + 1)$ corresponding to states with vibrational angular momentum $K = -v, -v + 2, \dots, v - 2, v$. Levels of the same v but different $|K|$ are in fact not quite degenerate. However, it should be appreciated that the anisotropy required to reach this “rigid” limit is very great, so that equation (64) will seldom be a good representation of the energy levels of real Van der Waals molecules.

For a case 3 complex with a non-linear equilibrium geometry, the situation is rather different. For an equilibrium angle $\theta = \pi/2$, the angular Hamiltonian may again be simplified

$$\begin{aligned}H &= b\hat{j}^2 + V(\theta) \\&\approx -b \left[\frac{\partial^2}{\partial \theta^2} + \frac{\partial^2}{\partial \alpha^2} \right] + V(\theta).\end{aligned}\tag{65}$$

Since the intermolecular potential is independent of the angle α , the angular Schrödinger equation is separable, with energy levels

$$E_{vK}^{\text{ang}} = E_v + bK^2.\tag{66}$$

The energy levels E_v are solutions of the one-dimensional equation

$$\left[-b \frac{d^2}{d\theta^2} + V(\theta) - E_v \right] \Phi_v(\theta) = 0.\tag{67}$$

In the limit of large anisotropy this may again be approximated by a harmonic oscillator, giving energy levels

$$E_{vK}^{\text{ang}} = V_0 + 2\sqrt{V_2 b}(v + \frac{1}{2}) + bK^2. \quad (68)$$

where V_2 is now the quadratic potential term in an expansion about $\theta = \pi/2$. For smaller anisotropies the solutions may be obtained by the Cooley method (section 2.1), although cyclic boundary conditions are required in the present case. The quantum number v describes the torsional oscillations of the diatom in the plane of the complex, while K is now a rotational angular momentum describing the free rotation of the diatom about the molecular axis.

For a rigid atom–diatom complex with equilibrium angle θ , the rotational part of the Hamiltonian may be written in the form [46]

$$H_{\text{rot}} = \frac{\hbar^2}{2} \sum_{\alpha\beta} [I^{-1}]_{\alpha\beta} \hat{J}_\alpha \hat{J}_\beta, \quad (69)$$

where I is the inertial tensor of the complex. Equation (69) may be rewritten in a form similar to that for an asymmetric top,

$$H_{\text{rot}} = A\hat{J}_a^2 + B\hat{J}_b^2 + C\hat{J}_c^2 + d_{ab}(\hat{J}_a\hat{J}_b + \hat{J}_b\hat{J}_a), \quad (70)$$

where

$$A \approx \langle \hbar^2 / (2\mu_{\text{mon}} r^2 \sin^2 \theta) + \hbar^2 / (2\mu R^2 \tan^2 \theta) \rangle \quad (71)$$

$$B \approx \langle \hbar^2 / 2\mu R^2 \rangle \quad (72)$$

$$C \approx \langle \hbar^2 / (2\mu R^2 + 2\mu_{\text{mon}} r^2) \rangle \quad (73)$$

$$d_{ab} = \langle \hbar^2 / 2\mu R^2 \tan \theta \rangle, \quad (74)$$

For an equilibrium geometry with $\theta = 90^\circ$, d_{ab} is identically zero, and the expectation values of equations (71) – (73) may be identified with the experimental rotational constants A , B and C . It may be noted that the equations for A and B are *not* the same as would be obtained by simply inverting I_{aa} and I_{bb} .

4.1.4 Transition between case 1 and case 2 coupling

The transition between case 1 and case 2 coupling is illustrated in Figure 3a, where the energy levels correlating with a diatom in its $j = 2$ state are plotted as a function of the V_2 anisotropy for $0 \leq J \leq 4$. The centre of the figure ($V_2 = 0$) corresponds to pure case 1 coupling, while the outer edges are near the case 2 limit. Several features may be noted:

- 1) The even and odd parity levels for a particular value of Ω become more nearly degenerate with increasing anisotropy, as the case 2 limit is approached. However, this happens much more quickly for the higher values of Ω . This is because the

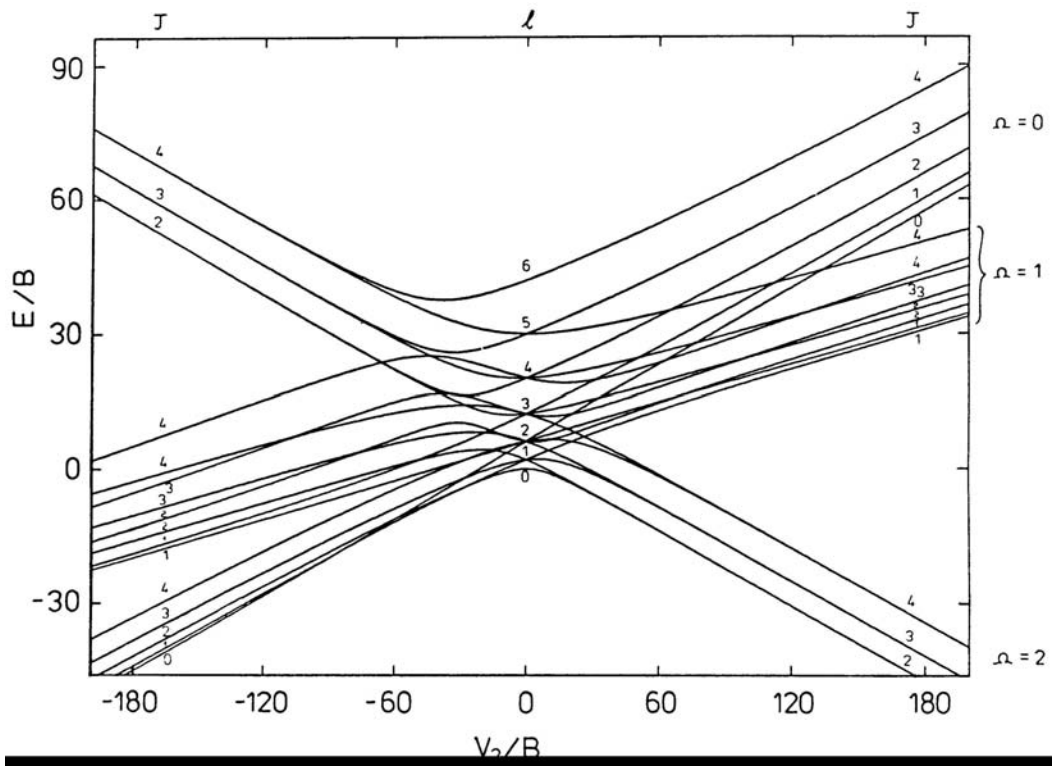


Figure 3a. The transition between coupling cases 1 and 2, caused by a $V_2P_2(\cos\theta)$ anisotropy. The diagram shows the energy levels for $j = 2$, $0 \leq J \leq 4$ as a function of V_2 .

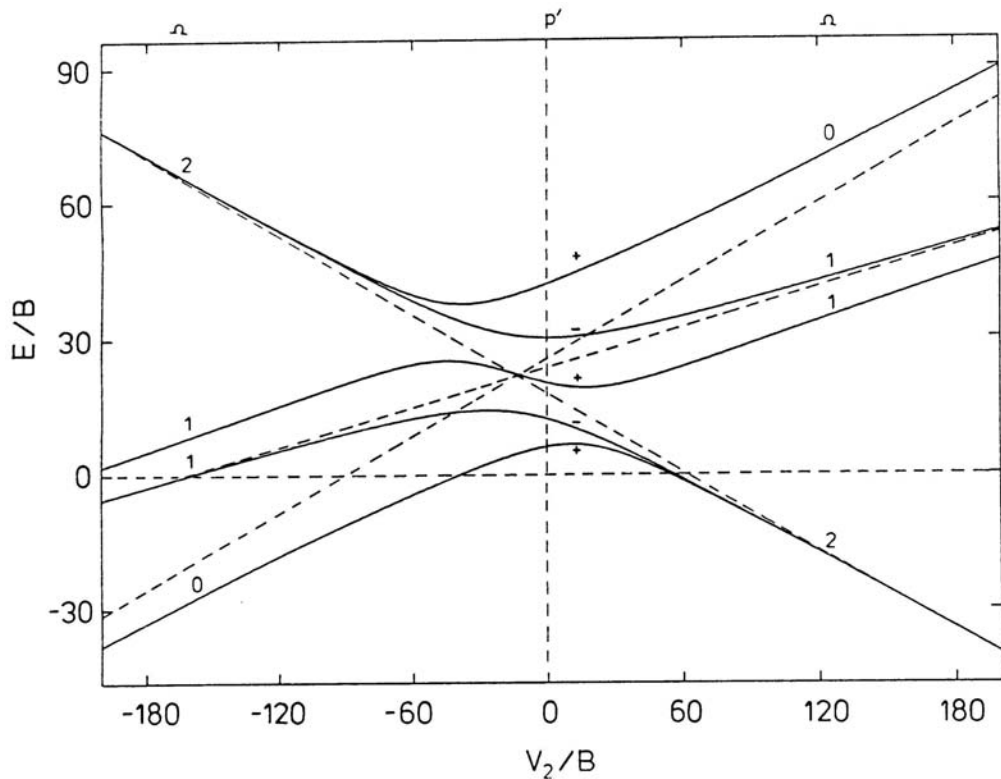


Figure 3b. The transition between coupling cases 1 and 2, caused by a $V_2P_2(\cos\theta)$ anisotropy. The diagram shows the energy levels for $j = 2$, $J = 4$ only as a function of V_2 .

essential difference between the even and odd parity manifolds is the existence of the $\Omega = 0$ state for $(-)^J$ (e) parity only. The other levels of this parity are shifted by coupling to this state via the Coriolis terms in the Hamiltonian, and the low Ω levels are shifted most because they are more directly coupled to $\Omega = 0$.

- 2) The energy level pattern may be regarded as originating from avoided crossings between pure case 2 states, which are themselves linearly dependent on the V_2 anisotropy coefficient. This is more clearly seen in Figure 3b, where only the $J = 4$ levels are shown; the dotted straight lines show the unperturbed positions of the pure case 2 states. The $\Omega = 0$ and 1^+ states interact strongly via Coriolis coupling, and are shifted furthest from the unperturbed positions.

4.1.5 Transition between case 2 and case 3 coupling

The transition between case 2 and case 3 coupling may be achieved by a V_1 or V_2 anisotropy (or any linear combination of the two). The correlation diagrams for pure V_1 and V_2 anisotropies are shown in Figures 4a and 4b. The two diagrams are qualitatively different:

- 1) For a V_1 anisotropy of either sign, the equilibrium geometry is linear. The high-anisotropy levels are thus those of a two-dimensional harmonic oscillator, as discussed above. The $j = 0$ level correlates with $v = 0$, while the $\Omega = 0$ and 1 components of $j = 1$ correlate with $v = 2$, $\Omega = 0$ and $v = 1$, $\Omega = 1$ respectively. The different Ω levels for $v \geq 2$ remain non-degenerate even at very high anisotropy, and for $v > 4$ it is quite difficult to assign the quantum numbers of the near-rigid limit. This illustrates the general point that case 2 coupling persists to much higher anisotropies for excited internal rotor (j) states than for the ground state.
- 2) For a V_2 anisotropy, the equilibrium structure depends on the sign of V_2 : it is linear for $V_2 < 0$ and T-shaped for $V_2 > 0$. The correlation diagram is thus unsymmetrical, with a level structure resembling that for V_1 on the left but a quite different structure on the right. However, since a negative V_2 gives a symmetric double well, all the levels of the V_1 case are doubled, separated by a tunnelling splitting which decreases as the anisotropy (which provides the barrier to tunnelling) increases. The tunnelling doubling is quenched if an additional V_1 anisotropy is introduced, making the two wells non-equivalent. The levels on the right of the diagram, by contrast, show the energy level pattern of equation (68): there is a set of approximately equally spaced vibrational levels, each of which has built upon it a stack of Ω (K) levels with a separation determined by the diatom rotational constant b .

4.1.6 Ar–HCl as a prototype system

The Van der Waals complex whose excited states have been studied in most detail is Ar–HCl, and it is interesting to consider it in some detail. The potential energy surface for this system has been through several cycles of refinement as better and better

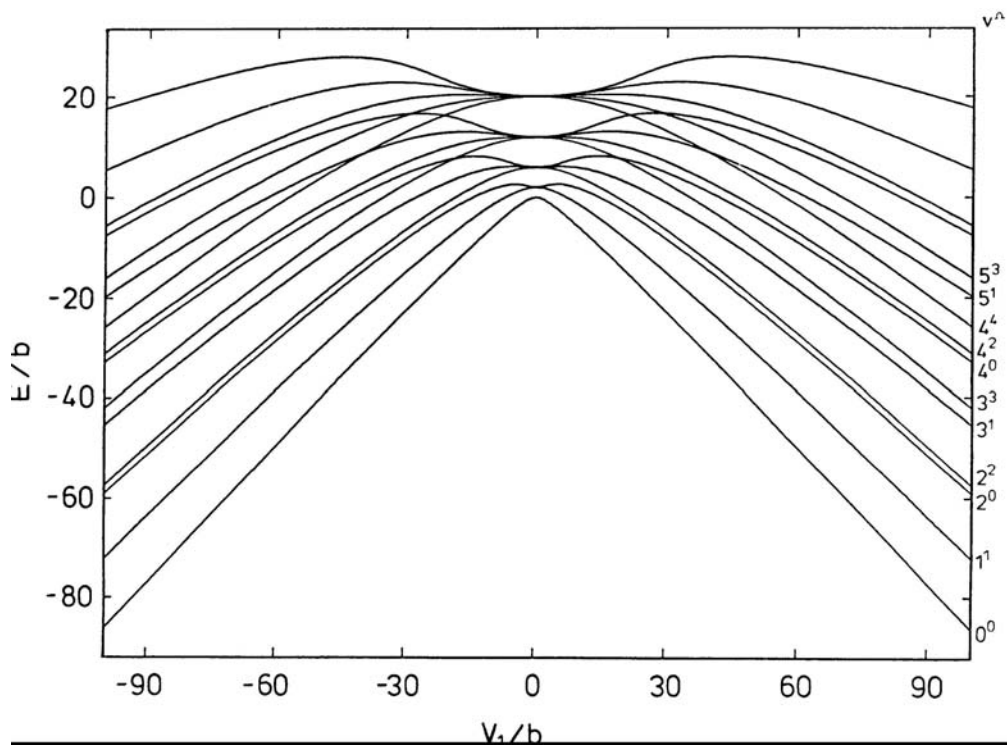


Figure 4a. The transition between coupling cases 2 and 3, caused by a $V_1 P_1(\cos \theta)$ anisotropy. The diagram shows the energy levels correlating with diatom free-rotor states with $j \leq 4$, calculated using a basis set including j values up to 12.

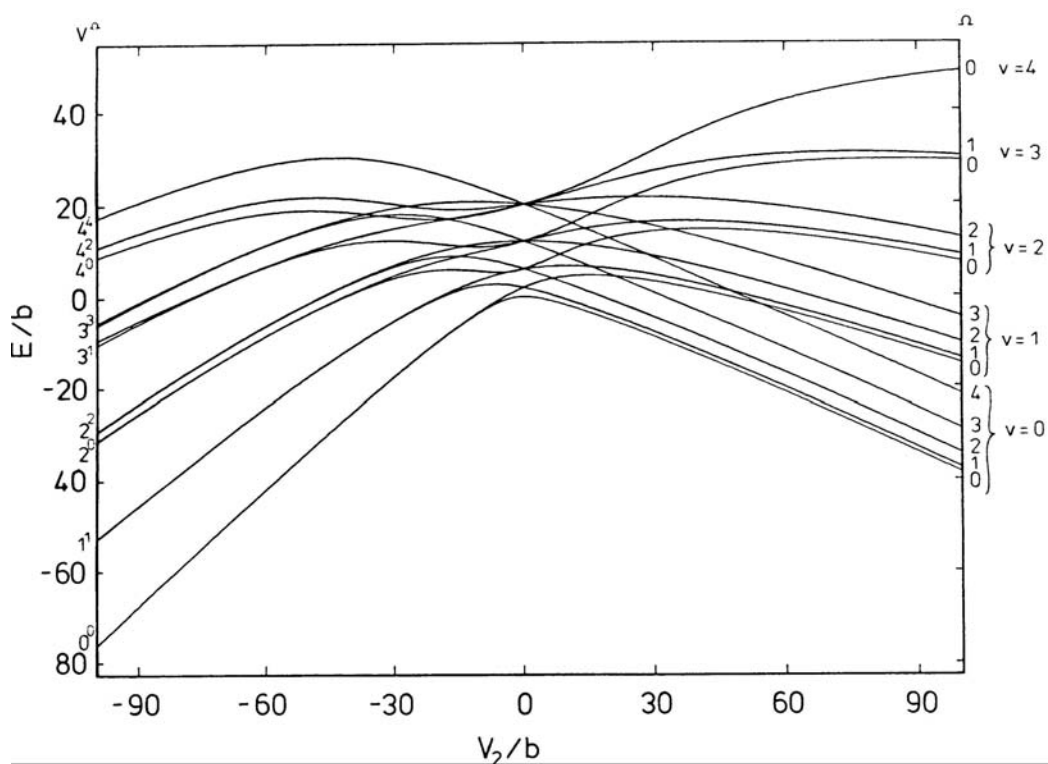


Figure 4b. The transition between coupling cases 2 and 3, caused by a $V_2 P_2(\cos \theta)$ anisotropy. The diagram shows the energy levels correlating with diatom free-rotor states with $j \leq 4$, calculated using a basis set including j values up to 12.

experimental information became available. At each stage, the predictions obtained from the best-fit potential have been useful in guiding further experiments.

The first reasonably accurate potential was that of Holmgren *et al.* [47], who determined an anisotropic potential by least-squares fitting of a parameterised form to molecular beam microwave and radiofrequency spectra of the Ar–HCl complex in its ground vibrational state. The resulting potential (potential IIb of ref. 47, designated the HWK potential here) had an absolute well depth of around 180 cm^{-1} , with a linear Ar–H–Cl equilibrium geometry. However, this potential was in marked disagreement with potentials determined from pressure broadening of HCl rotational lines by Ar [48,49], and was itself unable to reproduce the pressure broadening results. Accordingly, Hutson and Howard [50,51] obtained new potentials (the M3 and M5 potentials) by simultaneous fitting to molecular beam spectra, pressure broadening cross sections and second virial coefficients. The M3 and M5 potentials were quite similar to the HWK potential in the region of the absolute minimum, but had a much more anisotropic repulsive wall, which allowed them to model the pressure broadening results. However, the M3 and M5 potentials were quite different from one another in the region of the alternative linear geometry, Ar–Cl–H; the potential in this region had little effect on the calculated microwave and radiofrequency spectra, because the ground state bending wavefunction did not extend to high enough angles. This region of the potential was therefore not reliably determined by the data then available. Hutson and Howard [51] suggested that far-infrared spectroscopy would provide the most satisfactory diagnostic of the presence or absence of the secondary minimum, and gave calculated spectroscopic frequencies for the different potentials.

In the last few years, high-resolution far-infrared spectroscopy of Van der Waals complexes such as Ar–HCl has at last become experimentally feasible [52-58], using either laser Stark resonance or tunable far-infrared lasers. Near-infrared spectra of Ar–HCl have also been measured [59,45]; the vibrational frequencies for states of the complex correlating with HCl ($v = 1$) are very similar to those for states correlating with HCl ($v = 0$). The far-infrared spectra have been used to determine a new intermolecular potential (the H6(3) potential [60]) which is reliable over the whole range of angles.

The lowest few bending levels of Ar–HCl, calculated from the H6(3) potential using close-coupling calculations [60], are shown in Figure 5. The observed pattern may be compared with that expected for free rotation of the HCl (case 1 or 2) and for a near-rigid linear molecule (case 3). It may be seen immediately that the free-rotor picture is much closer to reality. Since the Ω quantum number is well-conserved, at least for low J , Ar–HCl is best viewed as a case 2 complex, with quantum numbers j , Ω , J and p' .

The most striking feature of Figure 5 is that the first excited Σ ($\Omega = 0$) state actually lies *below* the lowest Π ($\Omega = 1$) state. This is not at all the behaviour expected for a near-rigid molecule: in the language usually applied to linear triatomics, the Π state is the fundamental bending vibration, labelled 01^10 , and the Σ state is its overtone, labelled 02^00 . However, in the free-rotor (case 2) picture, both these states correlate with $j = 1$, and are expected to be degenerate except for the potential term $V_2g_2(jjK)$

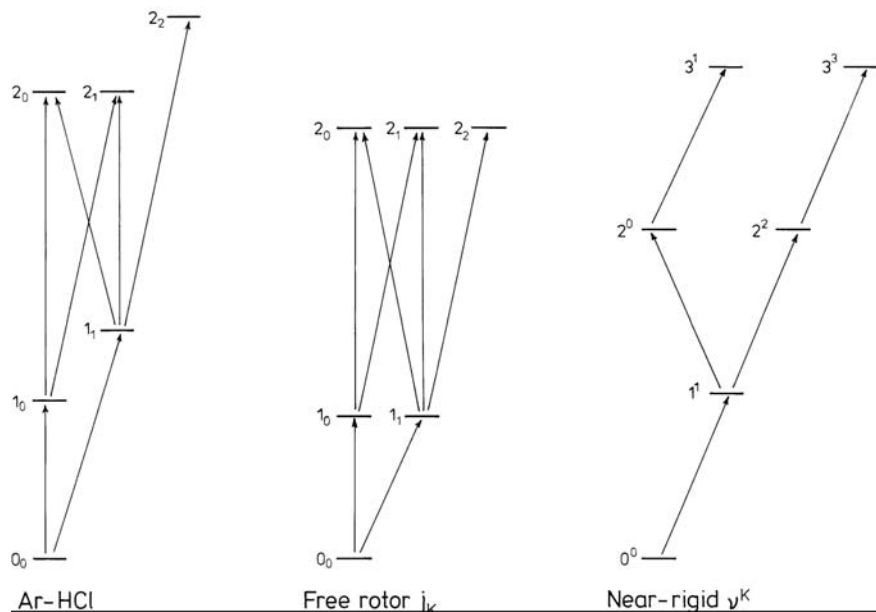


Figure 5. Bending energy levels of Ar–HCl, calculated using the H6(3) potential, and the patterns expected for a free internal rotor and for a semirigid linear molecule.

in equation (55). Since V_2 is negative in Ar–HCl, the Σ state lies below the Π state.

Ar–HCl also illustrates the changeover between case 2 and case 1 coupling. The $j = 1$, $\Omega = 0$ and 1 states discussed above are reasonably well separated, so that the Coriolis matrix elements between them can be treated by perturbation theory, at least at low J , although even here Lovejoy and Nesbitt [45] have found it necessary to go beyond perturbation theory at high J . In addition, because j is not in fact a good quantum number, there is a significant Coriolis matrix element between the first excited stretching state (nominally $j = 0$) and the Π bending state (nominally $j = 1$) which would not be present for pure case 2 coupling. Since these two states are only 1.5 cm^{-1} apart, the Coriolis mixing is quite substantial and results in the stretching band acquiring significant spectroscopic intensity.

Another consequence of the breakdown of the j quantum number is that the $\Delta j = \pm 1$ selection rule, which applies rigorously in free HCl, is only approximate in Ar–HCl. Thus the fundamental band in the near-infrared spectrum, which is nominally $j = 0 \leftarrow 0$, is of comparable intensity to the $j = 1 \leftarrow 0$ combination bands in the complex [45]. Similarly, bands of the complex corresponding to $j = 2 \leftarrow j = 0$ transitions are weakly allowed [60]. The $j = 2$ states also illustrate incipient case 1 coupling, because the $j = 2$, $\Omega = 0$ and 1 states are very close together (though the $\Omega = 2$ state is much further away). The $\Omega = 0$ and 1 states are thus thoroughly mixed by Coriolis coupling, and exhibit coupling intermediate between case 1 and case 2. A systematic theoretical study of the spectra of the rare gas – HCl complexes, using simulations of spectra to illustrate the effects of anisotropy on band positions and intensities, has been carried out by Clary and Nesbitt [41].

4.2 Centrifugal decoupling or helicity decoupling

One of the most useful approximations to the close-coupled equations is the centrifugal decoupling (CD) or helicity decoupling (HD) approximation [61,62]. This consists of neglecting the off-diagonal Coriolis terms in the body-fixed coupled equations, so that the coupled equations become diagonal in K . This is analogous to the coupled states (or centrifugal sudden) approximation of molecular scattering theory [63,64], although for bound states it is usual to include the diagonal Coriolis terms exactly, rather than approximating them as in coupled states calculations. The CD approximation factorises the large set of coupled equations for each J into a series of smaller sets for each allowed value of K . For high J and a given value of j_{\max} , it reduces the number of channels N from $(j_{\max} + 1)^2$ to $j_{\max} + 1 - K$. Since the computational effort involved in solving a set of coupled equations is proportional to N^3 , the CD approximation often provides considerable savings in computer time.

The CD approximation is appropriate for Van der Waals molecules exhibiting case 2 or case 3 coupling, where K is a good quantum number, but its results are significantly in error for case 1 complexes. Since all Van der Waals molecules exhibit case 1 coupling for sufficiently high rotational states, caution must be exercised in using the CD approximation for high values of J . An estimate of the validity of the CD approximation may be obtained by considering whether the condition (58) holds for the state of interest, using appropriate average values for B and V_2 .

Since the different K blocks are decoupled from one another in the CD approximation, and the angular coefficients $g_2(jj'K)$ are independent of the sign of K , states that differ only in the sign of K are degenerate in this approximation. Consequently, the parity-adapted linear combinations with $\Omega = |K|$ and $p = \pm 1$ (equation (41)) are also degenerate. This degeneracy is an artefact of the CD approximation, and does not hold for the exact solutions, although it is a good approximation for complexes exhibiting case 2 or case 3 coupling. The Coriolis terms may be included in a subsequent calculation step if necessary [65].

4.3 Distortion approximations

The CD approximation simplifies the coupled equations, but does not completely decouple them. The distortion approximations, on the other hand, neglect *all* the off-diagonal terms in the coupled equations, and thus result in uncoupled differential equations of the form

$$\left[-\frac{\hbar^2}{2\mu} \frac{d^2}{dR^2} + V_{va}(R) - E_{van} \right] \chi_{van}(R) = 0. \quad (75)$$

Distortion approximations may be obtained in either the space-fixed or body-fixed representations. The *space-fixed distortion* (SFD) approximation consists of neglecting all the off-diagonal potential terms in the space-fixed coupled equations (27). This gives the effective potential

$$V_{vjJ}^{\text{SFD}}(R) = (vjJ|V|vjJ) + \frac{\hbar^2 l(l+1)}{2\mu R^2} + E_{vj}^{\text{mon}}. \quad (76)$$

Conversely, the *body-fixed distortion* (BFD) approximation is obtained by neglecting all off-diagonal potential and Coriolis terms in the body-fixed coupled equations (39), giving

$$V_{vjKJ}^{\text{BFD}}(R) = (vjKJ|V|vjKJ) + \frac{\hbar^2}{2\mu R^2} [J(J+1) + j(j+1) - 2K^2] + E_{vj}^{\text{mon}}. \quad (77)$$

Equations (76) and (77) are simple one-dimensional Schrödinger equations identical in form to equation (6), and may be solved using the methods of section 2.1. All bound stretching (n) states for a particular (j, l, J) or (j, K, J) channel are taken to be supported by the same effective potential curve, which includes a centrifugal term and the diagonal matrix elements of the isotropic and anisotropic potentials. However, since only even order Legendre polynomials can have non-zero diagonal matrix elements, the distortion approximations completely neglect the effects of odd-order potential terms.

The distortion approximations are very simple to apply, and are valuable for providing preliminary estimates of the energy levels for a proposed potential surface, and for obtaining physical insight into the results of more accurate calculations. Space-fixed distortion calculations are reasonably accurate for case 1 complexes such as the rare gas–H₂ complexes, and body-fixed distortion calculations give a useful first estimate of the energy levels of case 2 complexes such as Ne–HCl. They are not usually adequate for quantitative work, and are not nowadays used much for atom–diatom systems, since coupled channel calculations are fairly cheap. However, analogous methods are sometimes used for larger systems, where coupled-channel calculations may be prohibitively expensive.

4.4 Perturbation theory

The distortion approximations neglect all the off-diagonal matrix elements in either the space-fixed or the body-fixed coupled equations. However, these neglected terms may be reintroduced by perturbation theory, using the wavefunctions of the distortion approximations as the zeroth order states. Representing the distortion eigenfunctions by the kets $|van\rangle$, where a collectively represents the angular quantum numbers (j, Ω, J, p) or (j, l, J, p) , we have

$$\psi_{van} = \psi_{van}^{(0)} + \sum'_{v'a'n'} \frac{\langle van|H'|v'a'n'\rangle}{E_{van}^{(0)} - E_{v'a'n'}^{(0)}} \psi_{v'a'n'}^{(0)}, \quad (78)$$

$$E_{van} = E_{van}^{(0)} + \sum'_{v'a'n'} \frac{|\langle van|H'|v'a'n'\rangle|^2}{E_{van}^{(0)} - E_{v'a'n'}^{(0)}}. \quad (79)$$

The perturbation Hamiltonian H' contains all the off-diagonal terms in the coupled equations. Note that there is no first-order correction to the energy in either the SFD or the BFD case, since all the diagonal terms are included in zeroth order. These equations

are readily generalised to higher order, but it is usually found that the results converge slowly, if at all, beyond second order.

A special problem for Van der Waals complexes is that, since there are relatively few stretching states n , the set of zeroth-order bound states $|van\rangle$ may not be sufficiently complete for the sum to converge. In physical terms, this means that the perturbation correction to the wavefunction has significant contributions from continuum states. A method for circumventing this problem, based on solving inhomogeneous differential equations instead of using the summation over the zeroth-order solutions, has been described by Hutson and Howard [66].

4.5 Adiabatic approximations

It is also possible to decouple the problem by performing an adiabatic or Born-Oppenheimer separation with respect to one coordinate, usually R . In this approximation, the wavefunction is written in the single product form

$$\psi_{an}^{\text{BO}}(\mathbf{R}, \mathbf{r}) = r^{-1} R^{-1} \Phi_a(\hat{\mathbf{R}}, \mathbf{r}; R) \chi_{an}^{\text{BO}}(R), \quad (80)$$

where the functions $\Phi_a(\hat{\mathbf{R}}, \mathbf{r}; R)$ are eigenfunctions of the fixed- R Hamiltonian with eigenvalues $U_a(R)$,

$$\left[H_{\text{mon}} + \frac{\hbar^2 \hat{l}^2}{2\mu R^2} + V(R, r, \theta) - U_a(R) \right] \Phi_a(\hat{\mathbf{R}}, \mathbf{r}; R) = 0. \quad (81)$$

If the effect of the radial kinetic energy operator on the functions $\Phi_a(\hat{\mathbf{R}}, \mathbf{r}; R)$ is neglected, the wavefunctions and energies are the solutions of the single-channel equation

$$\left[-\frac{\hbar^2}{2\mu} \frac{d^2}{dR^2} + U_a(R) - E_{an}^{\text{BO}} \right] \chi_{an}^{\text{BO}}(R) = 0. \quad (82)$$

The eigenvalues of the fixed- R Hamiltonian thus provide a set of effective potentials (adiabats) $U_a(R)$ for the stretching motion. The method used is to solve the fixed- R equation (81) on a grid of R values, and then to solve the resulting one-dimensional equations for $\chi_{an}^{\text{BO}}(R)$ and E_{an}^{BO} . This approach was first applied to Van der Waals complexes by Levine *et al.* [67], using a space-fixed basis set, and subsequently rederived by Holmgren *et al.* [68] in a body-fixed basis set. The body-fixed formulation has the major advantage that the Coriolis coupling terms can be neglected in equation (81), giving adiabatic curves with fewer avoided crossings. The criterion for validity of the adiabatic approximation is that the angular functions $\Phi_a(\hat{\mathbf{R}}, \mathbf{r}; R)$ should be slowly-varying functions of R : this does *not* necessarily require that the angular frequencies should be much faster than the stretching frequency. Adiabatic approximations are often quite accurate for the ground state of Van der Waals complexes, but become progressively less accurate for excited states, because of the presence of avoided crossings between different adiabatic curves.

It is not necessary to ignore the effect of the radial kinetic energy operator on the angular functions completely: both diagonal [68] and off-diagonal [69] corrections may be included if desired. A distinction which is sometimes made is that calculations in which no correction is included are termed Born-Oppenheimer calculations, whereas those in which the diagonal correction is included are termed adiabatic calculations.

An alternative adiabatic approximation is to carry out the separation with respect to the internal angular coordinate θ instead of R [51]; this has been termed the reversed Born-Oppenheimer approximation. In this approach, a one-dimensional stretching equation is first solved on a grid of θ values, and the eigenvalues of the fixed- θ equations provide an effective potential for the bending motion. The reversed Born-Oppenheimer approximation is particularly useful in obtaining qualitative insight into the nature of Van der Waals bending states, since it allows them to be considered independently of the stretching motions.

5. Dipole moments and spectroscopic intensities

Both the molecular Stark effect and the intensities of spectroscopic lines depend on matrix elements of the dipole moment operator between molecular eigenfunctions. The radial (R and r) parts of these integrals are straightforward to calculate once the wavefunctions are known, but the angular factors involved are quite complicated. This section will discuss the evaluation of the angular factors appearing in dipole moment matrix elements.

The dipole moment of a Van der Waals molecule is a vector function of the nuclear coordinates; thus for an atom-diatom Van der Waals molecule the dipole moment is denoted $\boldsymbol{\mu}(R, r)$. There may be contributions to $\boldsymbol{\mu}$ from 3 distinct sources:

- 1) The permanent dipole moments of the monomers
- 2) Dipole moments induced in one monomer by the electric field due to the non-spherical charge distribution of the other. *
- 3) Distortion of the electronic structure of the monomers due to “chemical” interactions such as electron overlap or charge transfer

For most Van der Waals molecules in their ground electronic states the dipole moment function is dominated by the first and second effects, although the third may become important at short range.

In order to investigate the properties of the dipole moment operator, it is convenient to expand the dipole moment function in terms of angular functions with well-defined angular momentum properties. This may be done in either space-fixed or body-fixed representations, as described in the following sections.

5.1 Space-fixed

The dipole moment vector of a Van der Waals molecule may be resolved into components along the space-fixed X , Y and Z directions. However, it is more convenient to

* Dispersion contributions to dipole moments are usually very small

Table 2. Symmetries of multipole moment contributions in atom–diatom Van der Waals molecules.

Origin	j	l	J
Direct dipole moment of diatom	1	0	1
Charge-induced dipole	0	1	1
Dipole-induced dipole	1	2	1
Quadrupole-induced dipole	2	3	1
Direct quadrupole moment of diatom	2	0	2

use linear combinations of these components

$$\begin{aligned}\mu_0 &= \mu_Z \\ \mu_{\pm 1} &= \mp \frac{1}{\sqrt{2}}(\mu_X \pm i\mu_Y).\end{aligned}\tag{83}$$

The $\mathcal{Y}_{jl}^{JM}(\hat{\mathbf{R}}, \hat{\mathbf{r}})$ functions of equation (23) form a complete basis set for the angular coordinates in an atom–diatom system, so that the components of the $\boldsymbol{\mu}$ vector may be expanded in terms of them,

$$\mu_M(\mathbf{R}, \mathbf{r}) = \sum_{jl} \mu_{jl}^{\text{SF}}(R, r) \mathcal{Y}_{jl}^{1M}(\hat{\mathbf{R}}, \hat{\mathbf{r}}).\tag{84}$$

The summation may be restricted to terms with $J = 1$ because $\boldsymbol{\mu}$ must transform as a vector with respect to rotations of the space-fixed axes, and to terms with $(j + l)$ odd since the dipole moment function has odd parity. Permanent and induced dipole moments in atom–diatom Van der Waals molecules are very simply expressed in the space-fixed representation, and the symmetries of the most commonly encountered terms are given in Table 2.

The matrix elements of these expansion functions between space-fixed basis functions may be obtained from the Wigner-Eckart theorem [9,70]

$$\begin{aligned}(j_i l_i J_i M_i | \mathcal{Y}_{j_l}^{1M} | j_f l_f J_f M_f) \\ = (-)^{j_i + l_i + J_i + M_i} \begin{pmatrix} J_i & 1 & J_f \\ -M_i & M & M_f \end{pmatrix} \\ \times [3(2J_i + 1)(2J_f + 1)(2j_i + 1)(2j_f + 1)(2l_i + 1)(2l_f + 1)]^{\frac{1}{2}} \\ \times \begin{pmatrix} j_i & j & j_f \\ 0 & 0 & 0 \end{pmatrix} \begin{pmatrix} l_i & l & l_f \\ 0 & 0 & 0 \end{pmatrix} \begin{pmatrix} J_i & J_f & 1 \\ j_i & j_f & j \\ l_i & l_f & l \end{pmatrix}.\end{aligned}\tag{85}$$

Since the dipole moment function has odd parity, it has no non-zero diagonal matrix elements. In addition, the $3j$ -symbols with zero projections ensure that the off-diagonal matrix elements are zero unless

- 1) Triangle relationships are satisfied by (j_i, j, j_f) and (l_i, l, l_f) .
- 2) $(j_i + j + j_f)$ and $(l_i + l + l_f)$ are both even.

The matrix element is also zero if $|J_i - J_f| > 1$, because of the triangle relationship for the $3j$ -symbol involving the total angular momentum.

Equation (85) immediately gives the spectroscopic selection rules for atom–diatom Van der Waals molecules exhibiting case 1 coupling. For the Ar-H₂ complex, for example, the transition moment is dominated by the dipole moment induced on Ar by the quadrupole moment of H₂. The quadrupole-induced dipole transforms as \mathcal{Y}_{23}^1 (Table 2), so that the selection rules are

$$\begin{aligned}\Delta J &= 0, \pm 1 \\ \Delta j &= 0, \pm 2 \\ \Delta l &= \pm 1, \pm 3.\end{aligned}\tag{86}$$

These selection rules rely on two assumptions:

- 1) The contributions from dipole moments due to other sources must be small.
- 2) The j and l quantum numbers must provide a good description of the wavefunctions.

Both these assumptions are valid for Ar-H₂, which is a weakly anisotropic system near the case 1 limit. However, it is important to realise that space-fixed selection rules such as these are *not* applicable to Van der Waals molecules exhibiting coupling cases 2 or 3.

5.2 Body-fixed

For Van der Waals molecules following case 2 or case 3 quantisation, it is more convenient to represent the dipole moment function in terms of the body-fixed functions of equation (32). The dipole moment is expanded

$$\mu_M(\mathbf{R}, \mathbf{r}) = \sum_{jK} \mu_{jK}^{\text{BF}}(R, r) \Phi_{jK}^{1M}(\hat{\mathbf{R}}, \hat{\mathbf{r}}).\tag{87}$$

Once again, the summation includes only functions with $J = 1$ and odd parity because of the requirement that $\boldsymbol{\mu}$ transform as a vector in the space-fixed axis system.

The space-fixed and body-fixed basis functions are related by equations (42) and (43). These may readily be inverted to obtain the relationship between the body-fixed and space-fixed coefficients

$$\mu_{jK}^{\text{BF}}(R, r) = \sum_l (-)^{j-l-K} (2l+1)^{\frac{1}{2}} \begin{pmatrix} j & l & 1 \\ K & 0 & -K \end{pmatrix} \mu_{jl}^{\text{SF}}(R, r).\tag{88}$$

The matrix elements of the $\Phi_{jK}^{1M}(\hat{\mathbf{R}}, \hat{\mathbf{r}})$ functions in the body-fixed representation are

$$\begin{aligned}
& (j_i K_i J_i M_i | \Phi_{jK}^{1M} | j_f K_f J_f M_f) \\
&= (4\pi)^{-1} (-)^{M_i - K_i} [3(2J_i + 1)(2J_f + 1)(2j_i + 1)(2j_f + 1)(2j + 1)]^{\frac{1}{2}} \\
&\times \begin{pmatrix} J_i & 1 & J_f \\ -K_i & K & K_f \end{pmatrix} \begin{pmatrix} J_i & 1 & J_f \\ -M_i & M & M_f \end{pmatrix} \\
&\times \begin{pmatrix} j_i & j & j_f \\ -K_i & K & K_f \end{pmatrix} \begin{pmatrix} j_i & j & j_f \\ 0 & 0 & 0 \end{pmatrix}.
\end{aligned} \tag{89}$$

For complexes containing dipolar monomers, the principal contribution to the transition dipole is just the monomer dipole moment, which has components with $j = 1$, $K = 0, \pm 1$. If j is a good quantum number for the complex (pure case 2 coupling), the resulting selection rules are

$$\begin{aligned}
\Delta J &= 0, \pm 1 \\
\Delta j &= \pm 1 \\
\Delta K &= 0, \pm 1.
\end{aligned} \tag{90}$$

In addition, the total parity of the wavefunction must change in a transition, so that only $e \leftrightarrow e$ and $f \leftrightarrow f$ transitions are allowed for $\Delta J = \pm 1$, and only $e \leftrightarrow f$ transitions for $\Delta J = 0$. The band structures are thus as expected for bending transitions in a linear molecule: $\Sigma \leftrightarrow \Sigma$ bands have P and R branches, while $\Sigma \leftrightarrow \Pi$ bands have P, Q and R branches; the P and R branches involve e levels of the Π state, while the Q branch involves f levels, which have a different rotational constant.

For real Van der Waals molecules, j is not a good quantum number, so that the selection rules above start to break down. In particular, it should be noted that they predict that the ‘‘fundamental’’ band, correlating with a pure vibrational transition of the monomer (i.e. $v, j = 1, 0 \leftarrow 0, 0$) should be forbidden (as it is for the free monomer). It is indeed true that, for weakly anisotropic systems such as Ne–HCl [71], the fundamental band is considerably weaker than the $1, 1 \leftarrow 0, 0$ bands. However, one effect of the anisotropy is to mix the j levels, and the fundamental band becomes allowed: for Ar–HCl, its intensity is comparable to that of the bending bands. For the same reason, bands such as $1, 2 \leftarrow 0, 0$ are also weakly allowed. There are also significant induced dipole terms in the transition moment, which can also cause the selection rules (90) to be relaxed.

Van der Waals stretching bands are also of importance. In principle, if the bending and stretching motions were independent, the stretching bands would acquire intensity only because the anisotropy of the intermolecular potential varies with R , so that the dipole moment of the complex is also a function of R . However, there is often quite strong mixing between bending and stretching states, and the stretching bands may borrow intensity from the bends. In Ar–HCl, for example, the lowest stretching state lies at 32.4 cm^{-1} , and is strongly mixed by Coriolis coupling to the Π bending state at

34.0 cm^{-1} . As a result, the stretching band has significant intensity. A similar effect occurs in Ar–HF [72], where the overtone of the Van der Waals stretch, $n = 2$, lies close to the Π bend and acquires intensity from it.

6. Larger systems

Although atom–diatom systems have been studied in most detail, there has also been some work on more complex systems. The principles governing the dynamics of such systems are similar to those for atom–diatom systems, but the angular momentum algebra is considerably more complicated. In addition, the number of possible coupling schemes is considerably greater. Again, most of the techniques used for Van der Waals complexes have direct analogues in the scattering literature. Three different classes of complex will be considered briefly here: atom–polyatom complexes, molecule–molecule complexes, and trimeric systems. A fuller account of the dynamics in such systems will be published separately [73].

A general feature of Van der Waals complexes is that they exhibit wide-amplitude motion, and are seldom well-described by near-rigid models. For larger systems, there are frequently a number of equivalent geometries which can be interchanged by vibrational motions. The resulting symmetries give rise to tunnelling splittings in the observed spectra. A major advantage of computational methods based on an expansion in free-rotor functions for the monomers is that these symmetries are taken into account in a natural way. However, even when the potential anisotropy is too strong for calculations based on monomer rotational functions to be feasible, the symmetries still exist and must be taken into account. Conventional group-theoretical methods, based solely on the point-group symmetry of the equilibrium geometry, are not adequate under such circumstances, and it is necessary to consider instead the complete molecular symmetry group arising from the permutation-inversion symmetry of the complex [74,75].

6.1 Atom–polyatom systems

Complexes formed from atoms and linear polyatomic molecules are very similar to atom–diatom systems: the coupled equations are identical, and the same angular momentum coupling schemes apply. The only added degree of complexity is that perpendicular vibrations of the polyatomic monomer are possible, and these introduce an extra quantum number (l or k) for the monomer vibrational angular momentum. Such states are analogous to those arising from $k > 0$ states of a symmetric top monomer, as discussed below.

Atom–nonlinear molecule complexes are of two basic types: atom–symmetric top and atom–asymmetric top. Several such complexes have been studied through their pure rotational spectra, but high-resolution infrared spectra, involving excitation of Van der Waals bending and stretching modes, are only just starting to become available [76]. There has also been a fair amount of theoretical work on the photodissociation spectra of such systems [77], but this has concentrated on the rates of photodissociation processes rather than on the energy level patterns.

As for atom–diatom complexes, three different angular momentum coupling schemes may be envisaged, and different sets of quantum numbers are appropriate in each case. The only system that has been studied in any detail is Ar–H₂O, which is close to the case 2 limit [78]: the anisotropy of the potential splits and shifts the H₂O free-rotor levels, but the free-rotor quantum numbers are still approximately conserved. Since H₂O is an asymmetric top, the energy level pattern is considerably more complicated than for an atom–diatom system, but can nevertheless be understood in terms of a similar physical picture.

Polyatomic hydrides are a special case in that they have quite large rotational constants. It is to be expected that most Van der Waals complexes involving non-hydride monomers will be much closer to the case 3 limit, and that their spectra will be best interpreted in terms of conventional near-rigid quantum numbers.

6.2 Molecule–molecule systems

The general molecule–molecule case, with two polyatomic fragments, has been very little studied. Brocks et al. [24] have derived the Hamiltonian for such a system in body-fixed coordinates, but have not performed actual calculations. This is a very important area, and high-resolution spectra are available for systems such as the H₂O dimer [79]. There has been a good deal of work on understanding these spectra, especially with regard to the symmetries of the states involved [80]. Coker and Watts [81] have simulated vibrational spectra of the water dimer using a semiempirical potential [82] obtained from a variety of experimental data. However, understanding the detailed spectroscopy and angular momentum coupling in such systems remains a research topic for the future.

There has been rather more work on the specific case of diatom–diatom systems, mostly aimed at understanding the spectrum of the HF dimer. For a diatom–diatom complex, there are three sources of angular momentum: the rotation of each of the monomers, characterised by quantum numbers j_1 and j_2 , and the end-over-end rotation of the complex as a whole. There are therefore many possible coupling schemes. The simplest is the fully space-fixed coupling scheme, in which j_1 and j_2 first couple to give a resultant j_{12} , which then couples with the end-over-end angular momentum l to give a resultant J , the total angular momentum. The Hamiltonian corresponding to this scheme is a straightforward generalisation of equation (11) [83,84] and this is the simplest representation in which to set up the coupled equations. Unfortunately, the space-fixed quantum numbers (j_1, j_2, j_{12}, l, J) bear little relationship to reality, so calculations in this representation are only meaningful if *all* the l channels for each (j_1, j_2, j_{12}, J) are included, and the number of such channels required for convergence is enormous.

There are at least two ways of formulating the diatom–diatom problem in body-fixed coordinates. In the first, j_1 and j_2 are each quantised along \mathbf{R} , with projections k_1 and k_2 . The total projection quantum number, $K = k_1 + k_2$, is nearly conserved, but the potential mixes basis functions with different k_1 and k_2 . This approach has been used by Barton and Howard [85], who performed adiabatic calculations on HF dimer and obtained an anisotropic intermolecular potential from microwave spectroscopic

data. Alternatively, the coupling of j_1 and j_2 to form j_{12} may be retained, but j_{12} is then quantised in the body-fixed frame with projection K along R . This approach has been used by Danby [37] in coupled-channel calculations on the H_2 dimer. There is no clear reason for preferring either of these formulations over the other: both provide a K quantum number, which is indeed a nearly good quantum number for $(\text{HF})_2$, but unfortunately neither k_1 and k_2 nor j_{12} is particularly useful in analysing the spectrum.

6.3 Trimeric systems

The study of the dynamics of trimeric Van der Waals systems is in its infancy, although there has been a lot of work on H_3^+ and its isotopic variants [86], which have some similarities with Van der Waals clusters, at least for their higher vibrational levels. Once again, for sufficiently strongly bound trimers, conventional near-rigid theory may be employed; the systems that cause difficulty are those for which internal rotations or exchange of identical monomers are feasible, so that conventional Hamiltonians involving an expansion about the equilibrium geometry are inappropriate.

The methods used for atom–diatom systems are not generally suitable for trimeric systems. For a system such as Ne_3 , there is little reason to treat one pair of Ne atoms differently from the third, and an expansion in Ne–Ne vibration-rotation functions $\phi_{vj}(r)$ as in equation (19) would not be expected to be quickly convergent. However, symmetrised normal coordinates are not suitable either, because such coordinate systems are usually not single-valued for all possible geometries. One possible way around this problem is to use hyperspherical coordinates [87], in which the three internal coordinates are chosen to be two angles and a hyperradius ρ rather than one angle and two distances. This allows the three-particle Schrödinger equation to be cast as a set of coupled differential equations in the hyperradius, and the same numerical techniques may be used as in the atom–diatom case. Frey and Howard [88-90] have attempted to solve the coupled equations by making an adiabatic separation with respect to ρ , and have included non-adiabatic corrections to the ground-state energy by perturbation theory. Hutson and Jain [91] have solved the coupled equations directly, using the log-derivative propagator. These methods are promising, but very demanding of computer time, and it has not yet been possible to include overall rotation of the complex.

Systems such as Ar_2HCl and Ar_2HF are of great interest, because they offer the hope of a spectroscopic determination of non-additive contributions to intermolecular potentials. Microwave spectra of these systems have been observed [92,93] and it should be possible to obtain infrared spectra. A complete solution of the dynamical problem for such systems is beyond our capabilities at present, but Hutson et al. [94] have carried out a preliminary study, investigating the hindered rotation of an HCl molecule under the influence of a (fixed) pair of Ar atoms. They concluded that infrared spectra of these systems *would* probably contain enough information to determine the effects of three-body forces. This is likely to be an important research topic in the future.

Acknowledgment

This work is supported by the Science and Engineering Research Council.

References

- [1] B. J. Howard, MTP International Review of Science, Series 2, Physical Chemistry 2 (1975) 93.
- [2] G. E. Ewing, Can. J. Phys. 54 (1976) 487.
- [3] R. J. Le Roy and J. S. Carley, Adv. Chem. Phys. 42 (1980) 353.
- [4] A. C. Legon and D. J. Millen, Chem. Rev. 86 (1986) 635.
- [5] D. J. Nesbitt, Chem. Rev. 88 (1988) 843.
- [6] A. D. Buckingham, P. W. Fowler and J. M. Hutson, Chem. Rev. 88 (1988) 963.
- [7] J. M. Hutson, Ann. Rev. Phys. Chem. 41 (1990) 123.
- [8] K. C. Janda, Adv. Chem. Phys. 60 (1985) 201.
- [9] D. M. Brink and G. R. Satchler, *Angular Momentum*: 2nd ed., Clarendon Press, Oxford (1968).
- [10] J. Tennyson and B. T. Sutcliffe, J. Chem. Phys. 77 (1982) 4061.
- [11] I. P. Hamilton and J. C. Light, J. Chem. Phys. 84 (1986) 306.
- [12] W. H. Press, B. P. Flannery, S. A. Teukolsky and W. T. Vetterling, *Numerical Recipes*: Cambridge University Press, Cambridge (1986).
- [13] J. W. Cooley, Math. Comput. 15 (1961) 363.
- [14] B. R. Johnson, J. Chem. Phys. 67 (1977) 4086.
- [15] B. R. Johnson, J. Comp. Phys. 13 (1973) 445.
- [16] D. E. Manolopoulos, J. Chem. Phys. 85 (1986) 6425; D. E. Manolopoulos, Ph. D. thesis, Cambridge University (1988).
- [17] J. M. Hutson, J. Phys. B 14 (1981) 851.
- [18] R. Rydberg, Z. Phys. 73 (1931) 326; Z. Phys. 80 (1933) 514; O. Klein, Z. Phys. 76 (1932) 226; A. L. G. Rees, Proc. Roy. Soc. (London) 59 (1947) 998.
- [19] J. Tellinghuisen, Comp. Phys. Commun. 6 (1974) 221.
- [20] M. S. Child and D. J. Nesbitt, Chem. Phys. Lett. 149 (1988) 404.
- [21] M. Abramowitz and I. A. Stegun, *Handbook of Mathematical Functions*: National Bureau of Standards (1965).
- [22] H. Kreek and R. J. Le Roy, J. Chem. Phys. 63 (1975) 338.
- [23] W.-K. Liu, J. E. Grabenstetter, R. J. Le Roy and F. R. McCourt, J. Chem. Phys. 68 (1978) 5028.
- [24] G. Brocks, A. van der Avoird, B. T. Sutcliffe and J. Tennyson, Mol. Phys. 50 (1983) 1025.
- [25] J. T. Hougen, J. Chem. Phys. 36 (1962) 519.
- [26] J. K. G. Watson, Mol. Phys. 19 (1970) 465.
- [27] J. H. van Vleck, Rev. Mod. Phys. 23 (1951) 213.
- [28] R. G. Gordon, J. Chem. Phys. 51 (1969) 14.
- [29] W. N. Sams and D. J. Kouri, J. Chem. Phys. 51 (1969) 4809; J. Chem. Phys. 51 (1969) 4815.
- [30] J. C. Light and R. B. Walker, J. Chem. Phys. 65 (1976) 4272; E. B. Stechel, R. B. Walker and J. C. Light, J. Chem. Phys. 69 (1978) 3518.
- [31] G. A. Parker, T. G. Schmalz and J. C. Light, J. Chem. Phys. 73 (1980) 1757.

- [32] M. H. Alexander, *J. Chem. Phys.* 81 (1984) 4510.
- [33] M. H. Alexander and D. E. Manolopoulos, *J. Chem. Phys.* 86 (1987) 2044.
- [34] A. M. Dunker and R. G. Gordon, *J. Chem. Phys.* 64 (1976) 4984.
- [35] B. R. Johnson, *J. Chem. Phys.* 69 (1978) 4678.
- [36] M. Shapiro and G. G. Balint-Kurti, *J. Chem. Phys.* 71 (1979) 1461.
- [37] G. Danby, *J. Phys. B* 16 (1983) 3393.
- [38] J. M. Hutson, *Chem. Phys. Lett.* 151 (1988) 565.
- [39] R. J. Le Roy and J. van Kranendonk, *J. Chem. Phys.* 61 (1974) 4750.
- [40] J. Tennyson, *Comp. Phys. Reports* 4 (1986) 1.
- [41] D. C. Clary and D. J. Nesbitt, *J. Chem. Phys.* 90 (1989) 7000.
- [42] Z. Bačić and J. C. Light, *J. Chem. Phys.* 85 (1986) 4594; *J. Chem. Phys.* 86 (1987) 3065.
- [43] S. Bratoz and M. L. Martin, *J. Chem. Phys.* 42 (1965) 1051.
- [44] G. C. Corey, R. J. Le Roy and J. M. Hutson, *Faraday Discuss. Chem. Soc.* 73 (1982) 339; J. M. Hutson and R. J. Le Roy, *J. Chem. Phys.* 83 (1985) 1107.
- [45] C. M. Lovejoy and D. J. Nesbitt, *Chem. Phys. Lett.* 146 (1988) 582.
- [46] J. A. Beswick, N. Halberstadt and J. M. Hutson, unpublished work (1988).
- [47] S.L. Holmgren, M. Waldman and W. Klemperer, *J. Chem. Phys.* 69 (1978) 1661.
- [48] A. M. Dunker and R.G. Gordon, *J. Chem. Phys.* 64 (1976) 354.
- [49] J. G. Kircz, G. J. Q. van der Peyl, J. van der Elsken and D. Frenkel, *J. Chem. Phys.* 69 (1978) 4606.
- [50] J. M. Hutson and B. J. Howard, *Mol. Phys.* 43 (1981) 493.
- [51] J. M. Hutson and B. J. Howard, *Mol. Phys.* 45 (1982) 769.
- [52] M. D. Marshall, A. Charo, H. O. Leung and W. Klemperer, *J. Chem. Phys.* 83 (1985) 4924.
- [53] D. Ray, R. L. Robinson, D.-H. Gwo and R. J. Saykally, *J. Chem. Phys.* 84 (1986) 1171.
- [54] R. L. Robinson, D.-H. Gwo, D. Ray and R. J. Saykally, *J. Chem. Phys.* 86 (1987) 5211.
- [55] R. L. Robinson, D.-H. Gwo and R. J. Saykally, *J. Chem. Phys.* 87 (1987) 5156.
- [56] R. L. Robinson, D.-H. Gwo and R. J. Saykally, *J. Chem. Phys.* 87 (1987) 5149.
- [57] R. L. Robinson, D.-H. Gwo and R. J. Saykally, *Mol. Phys.* 63 (1988) 1021.
- [58] K. L. Busarow, G. A. Blake, K. B. Laughlin, R. C. Cohen, Y. T. Lee and R. J. Saykally, *Chem. Phys. Lett.* 141 (1987) 289.
- [59] B. J. Howard and A. S. Pine, *Chem. Phys. Lett.* 122 (1985) 1.
- [60] J. M. Hutson, *J. Chem. Phys.* 89 (1988) 4550.
- [61] H. Klar, *Nuovo Cimento* 4A (1971) 529.
- [62] M. Tamir and M. Shapiro, *Chem. Phys. Lett.* 31 (1975) 166.
- [63] R. T Pack, *J. Chem. Phys.* 60 (1974) 633.
- [64] P. McGuire and D. J. Kouri, *J. Chem. Phys.* 60 (1974) 2488.
- [65] J. Tennyson and B. T. Sutcliffe, *Mol. Phys.* 58 (1986) 1067.
- [66] J. M. Hutson and B. J. Howard, *Mol. Phys.* 41 (1980) 1113.

- [67] R. D. Levine, *J. Chem. Phys.* 46 (1967) 331; *J. Chem. Phys.* 49 (1968) 51; R. D. Levine, B. R. Johnson, J. T. Muckerman and R. B. Bernstein, *J. Chem. Phys.* 49 (1968) 56.
- [68] S.L. Holmgren, M. Waldman and W. Klemperer, *J. Chem. Phys.* 67 (1977) 4414.
- [69] J. M. Hutson and B. J. Howard, *Mol. Phys.* 41 (1980) 1123.
- [70] A. M. Dunker and R. G. Gordon, *J. Chem. Phys.* 68 (1978) 700.
- [71] C. M. Lovejoy and D. J. Nesbitt, *Chem. Phys. Lett.* 147 (1988) 490.
- [72] C. M. Lovejoy, M. D. Schuder and D. J. Nesbitt, *J. Chem. Phys.* 85 (1986) 4890.
- [73] J. M. Hutson, in *Dynamics of Polyatomic Van der Waals Complexes*, ed. N. Halberstadt and K. C. Janda: Plenum, New York (1990).
- [74] H. C. Longuet-Higgins, *Mol. Phys.* 6 (1963) 445.
- [75] P. R. Bunker, *Molecular Symmetry and Spectroscopy*: Academic Press, New York (1979).
- [76] R. C. Cohen, K. L. Busarow, K. B. Laughlin, G. A. Blake, M. Havenith, Y. T. Lee and R. J. Saykally, *J. Chem. Phys.* 89 (1988) 4494.
- [77] J. M. Hutson, D. C. Clary and J. A. Beswick, *J. Chem. Phys.* 81 (1984) 4474; A. C. Peet, D. C. Clary and J. M. Hutson, *J. Chem. Soc., Faraday Trans. II* 83 (1987) 1719.
- [78] J. M. Hutson, *J. Chem. Phys.* 92 (1990) 157.
- [79] G. T. Fraser, R. D. Suenram and L. H. Coudert *J. Chem. Phys.* 90 (1989) 6077 and references therein.
- [80] L. H. Coudert and J. T. Hougen, *J. Mol. Spectrosc.* 130 (1988) 86.
- [81] D. F. Coker and R. O. Watts, *J. Phys. Chem.* 91 (1987) 2513.
- [82] J. R. Reimers, R. O. Watts and M. L. Klein, *Chem. Phys.* 64 (1982) 95.
- [83] H. Klar, *Z. Phys.* 228 (1969) 59.
- [84] M. H. Alexander and A. E. DePristo, *J. Chem. Phys.* 66 (1977) 2166.
- [85] A. E. Barton and B. J. Howard, *Faraday Discuss. Chem. Soc.* 73 (1982) 45.
- [86] J. Tennyson and B. T. Sutcliffe, *Mol. Phys.* 51 (1984) 887; *Mol. Phys.* 54 (1985) 141; *Mol. Phys.* 56 (1985) 1175; *Mol. Phys.* 58 (1986) 1067.
- [87] B. R. Johnson, *J. Chem. Phys.* 79 (1983) 1916.
- [88] J. G. Frey and B. J. Howard, *Chem. Phys.* 99 (1985) 415.
- [89] J. G. Frey and B. J. Howard, *Chem. Phys.* 99 (1985) 427.
- [90] J. G. Frey, *Mol. Phys.* 65 (1988) 1313.
- [91] J. M. Hutson and S. Jain, *J. Chem. Phys.* 91 (1989) 4197.
- [92] H. S. Gutowsky, T. D. Klots, C. Chuang, C. A. Schmuttenmaer and T. Emilsson, *J. Chem. Phys.* 86 (1987) 569.
- [93] T. D. Klots, C. Chuang, R. S. Ruoff, T. Emilsson and H. S. Gutowsky, *J. Chem. Phys.* 86 (1987) 5315.
- [94] J. M. Hutson, J. A. Beswick and N. Halberstadt, *J. Chem. Phys.* 90 (1989) 1337.